ISDE International Lectures

The 8th ISDE International Lectures

Remote Sensing and Geoinformation for Natural Hazards Management and Disaster Mitigation

January 23, 2024

Organizer:
International Society for Digital Earth(ISDE)

Co-organizer:
Research Center for Digital Mountain and Remote Sensing Application,
Institute of Mountain Hazards and Environment, CAS

Supporters:
International Research Center of Big Data for Sustainable Development Goals
International Journal of Digital Earth
Big Earth Data

International Society for Digital Earth

ISDE International Lectures

The 8th ISDE International Lectures

Theme	Remote Sensing and Geoinformation for Natural Hazards Management and Disaster Mitigation
Date and Time	January 23, 2024, 13:30 - 15:00 (CET)
Organized by	International Society for Digital Earth
Co-organized by	Research Center for Digital Mountain and Remote Sensing Application, Institute of Mountain Hazards and Environment, CAS
Supported by	International Research Center of Big Data for Sustainable Development Goals International Journal of Digital Earth Big Earth Data
Online	Zoom ID: 861 3702 7671, Password: 110945

Invited Speakers

Bakhtiar Feizizadeh
University of Tabriz, Iran & University of Münster, Germany

Topic:An Integrated Geoinformation-based Methodology for Spatiotemporal Modelling of the Environmental Impacts of Climate Change in Dying Lakes Basins

Meisam Amani
WSP Environment and Infrastructure Canada Limited, Canada

Topic:Wetland Mapping and Change Analysis in Canada Using Advanced AI and Remote Sensing Techniques

Sadra Karimzadeh
University of Tabriz, Iran & Tokyo Institute of Technology, Japan

Topic:Remote Sensing of Vulnerability: Damage Estimation of Karmanmaras Earthquake in Turkey 2023

Contact: ISDE Secretariat
Email: isde@radi.ac.cn Tel.: 86-10-82178912

Welcome to visit ISDE website: www.digitalearth-isde.org

The 8th ISDE International Lectures

ISDE International Lectures

Remote Sensing and Geoinformation for Natural Hazards Management and Disaster Mitigation

January 23, 2024

Programme

13:30-13:35	**Welcome and Introduction** **Moderator: Bakhtiar Feizizadeh**
13:35-13:55	**Topic: An Integrated Geoinformation-based Methodology for Spatiotemporal Modelling of the Environmental Impacts of Climate Change in Dying Lakes Basins** **Speaker: Bakhtiar Feizizadeh (University of Münster, Germany)**
13:55-14:15	**Topic: Wetland Mapping and Change Analysis in Canada Using Advanced AI and Remote Sensing Techniques** **Speaker: Meisam Amani (WSP Environment and Infrastructure Canada Limited, Canada)**
14:15-14:35	**Topic: Remote Sensing of Vulnerability: Damage Estimation of Karmanmaras Earthquake in Turkey 2023** **Speaker: Sadra Karimzadeh (University of Tabriz, Iran; Tokyo Institute of Technology, Japan)**
14:35-14:57	**Group Photo** **Q&A**
14:57-15:00	**Announcement of the 9th ISDE International Lectures**

ISDE International Lectures

Welcome to share your thoughts and questions with us !

Contact: ISDE Secretariat
Email: isde@radi.ac.cn
Tel.: 86-10-82178912
Website: http://www.digitalearth-isde.org
@isde_digitalearth
@International Society for Digital Earth
@International Society for Digital Earth

ISDE LinkedIn

ISDE WeChat (in

An Integrated Geoinformation-based Methodology for Spatiotemporal Modelling of the Environmental Impacts of Climate Change in Dying Lakes Basins

Bakhtiar Feizizadeh

Department of Remote Sensing and GIS, University of Tabriz, Iran

Institute of Geoinfomatic, University of Munster, Germany

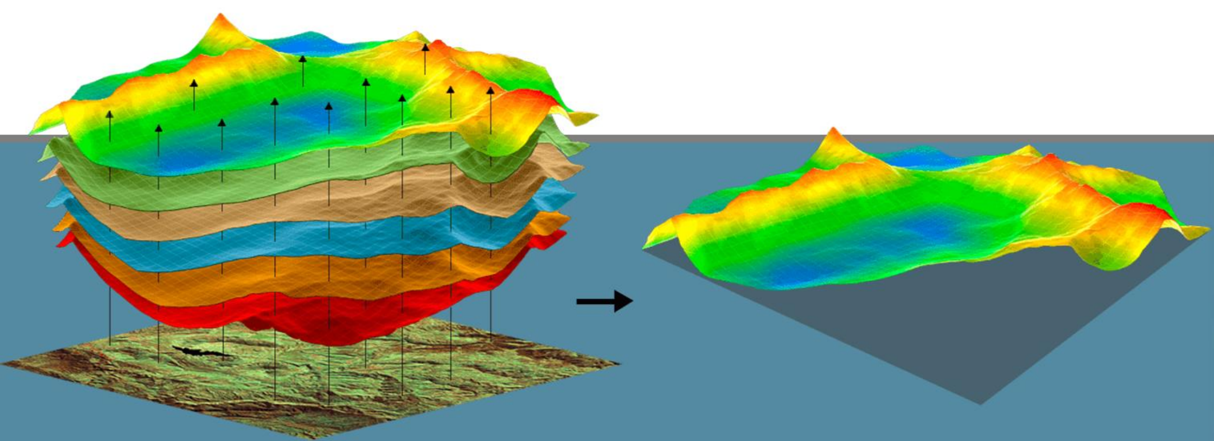

- 2000 – 2004: Bachelor in Geography, University of Tabriz

- 2004 – 2006: Master in Remote Sensing and GIS, University of Tabriz

- 2010 – 2014: University of Salzburg, Department of Geoinformatics (Z-GIS), Salzburg, Austria, Supervised by Prof.Dr. Thomas Blaschke, PhD thesis topic: “Uncertainty, Sensitivity and Fuzzy Sets in GIS Multi-Criteria Decision Analysis”

- 201۲ – 201۳: San Diego State University (SDSU), Department of GIScince, California, USA

- 201۴ – 2018: Assistant professor & 2018-2020 as associated professor in the Department of Remote Sensing and GIS, & Deputy Director of Institute of Environment, University of Tabriz, Iran
- 2020– 20۲2: experienced researcher in applied Geoinformation lab, Department of Geography, Humboldt University of Berlin

ifgi, University of Munster: Since February 2023




A research project funded by Alexander Humboldt Foundation

Scenario-based spatial modeling of land use/cover change effects on food security: the case of the Lake Urmia drought

4.2021- 1.2023

Humboldt University of Berlin

HUMBOLDT-UNIVERSITÄT ZU BERLIN

UNIVERSITÄT SALZBURG

Z_GIS

Alexander von Humboldt
Stiftung / Foundation

Prof. Tobia Lakes

Dr.Mohessn Makki

Dr. Robert Kitzmann

Prof. Patrick Hostert

Prof. Thomas Blaschke

Prof. Ayoob Sahrifi

Climate change and its environmental impacts

- ✓ Climate change has resulted in several environmental challenges that threaten the wellbeing of humans and wildlife alike.
- ✓ Droughts are one of the most tangible impacts of climate change as they affect water availability, food production, ecosystem services, and can potentially trigger conflicts between stakeholders.

Climate change and its environmental impacts

- As this figure shows, global temperature has increased by about 4 C over the past 50 years.

- The researchers indicated that the results underscore the "*need for immediate action*" to avoid even greater warming.

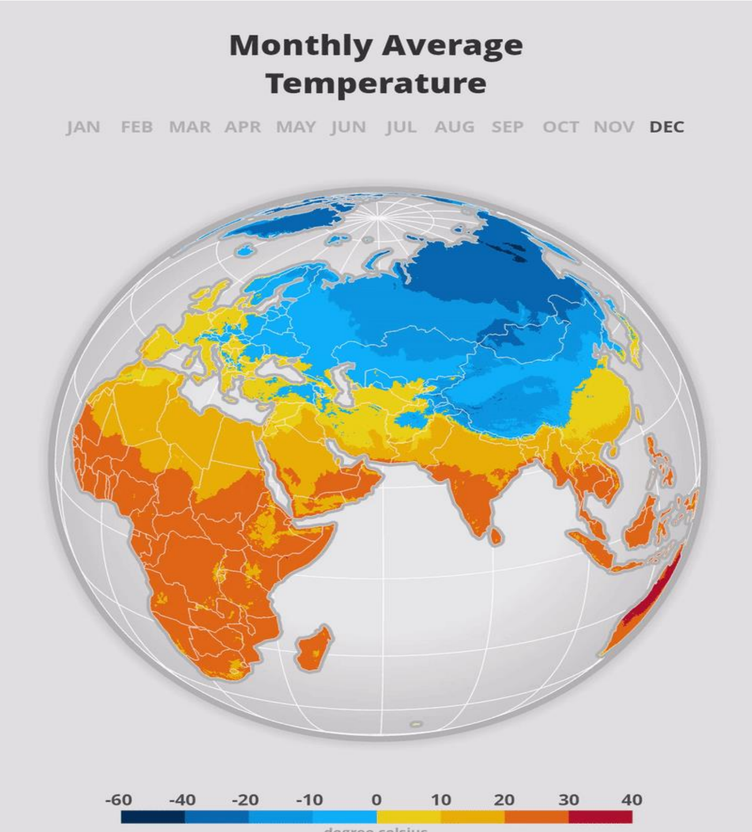

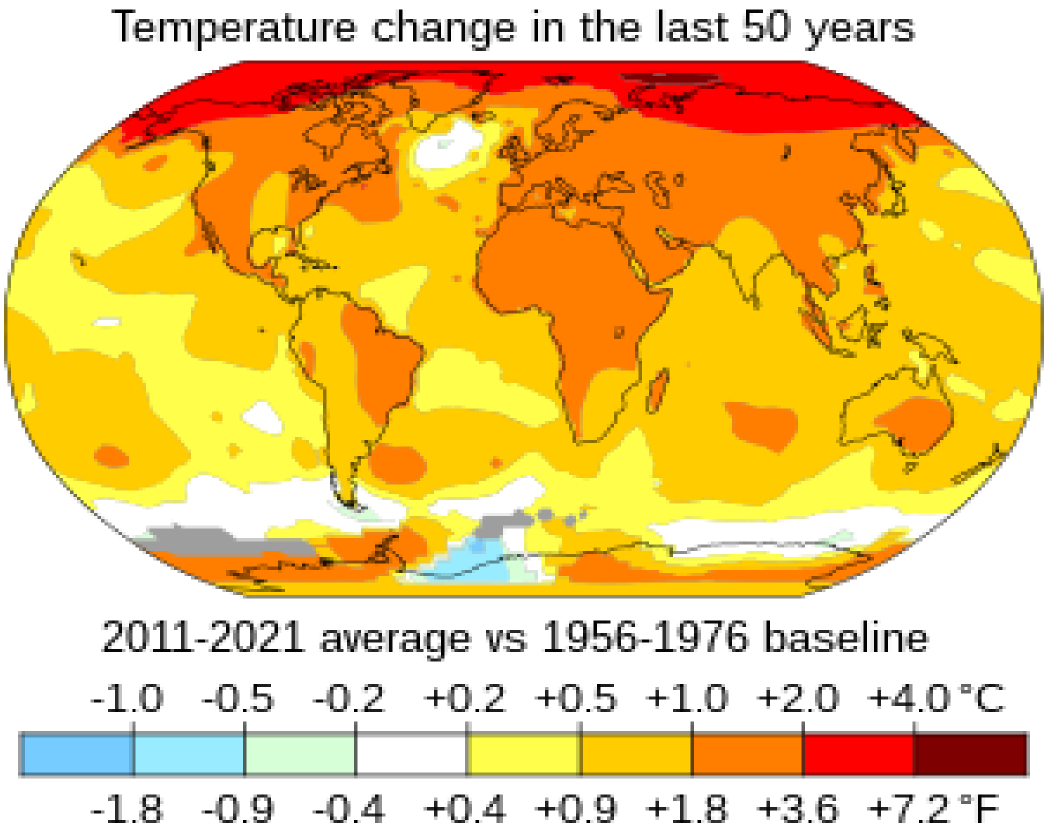

Climate change and the issue of dying lakes

- One of the most tangible environmental impacts of climate change can be observed in the environments of dying lakes.
- The 140 lakes comprising about 69% of the Earth's freshwater habitats are threatened by climate change (Neumannl, 2021).
- Changes in thermal habitats as a result of climate change can have a variety of significant environmental impacts on dying lakes.

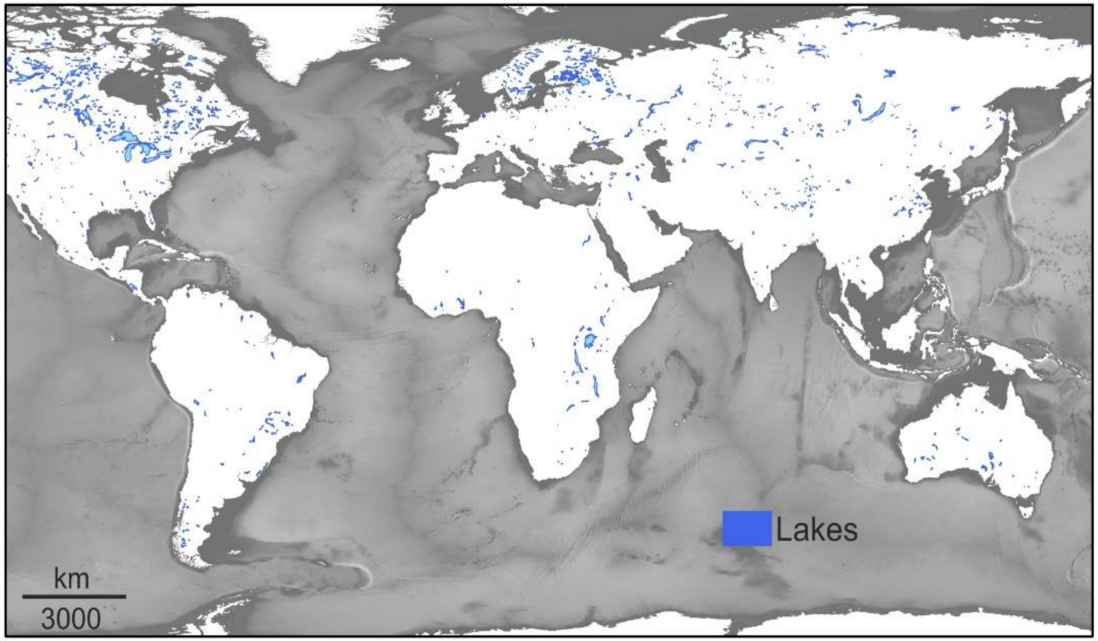

Urmia lake drought

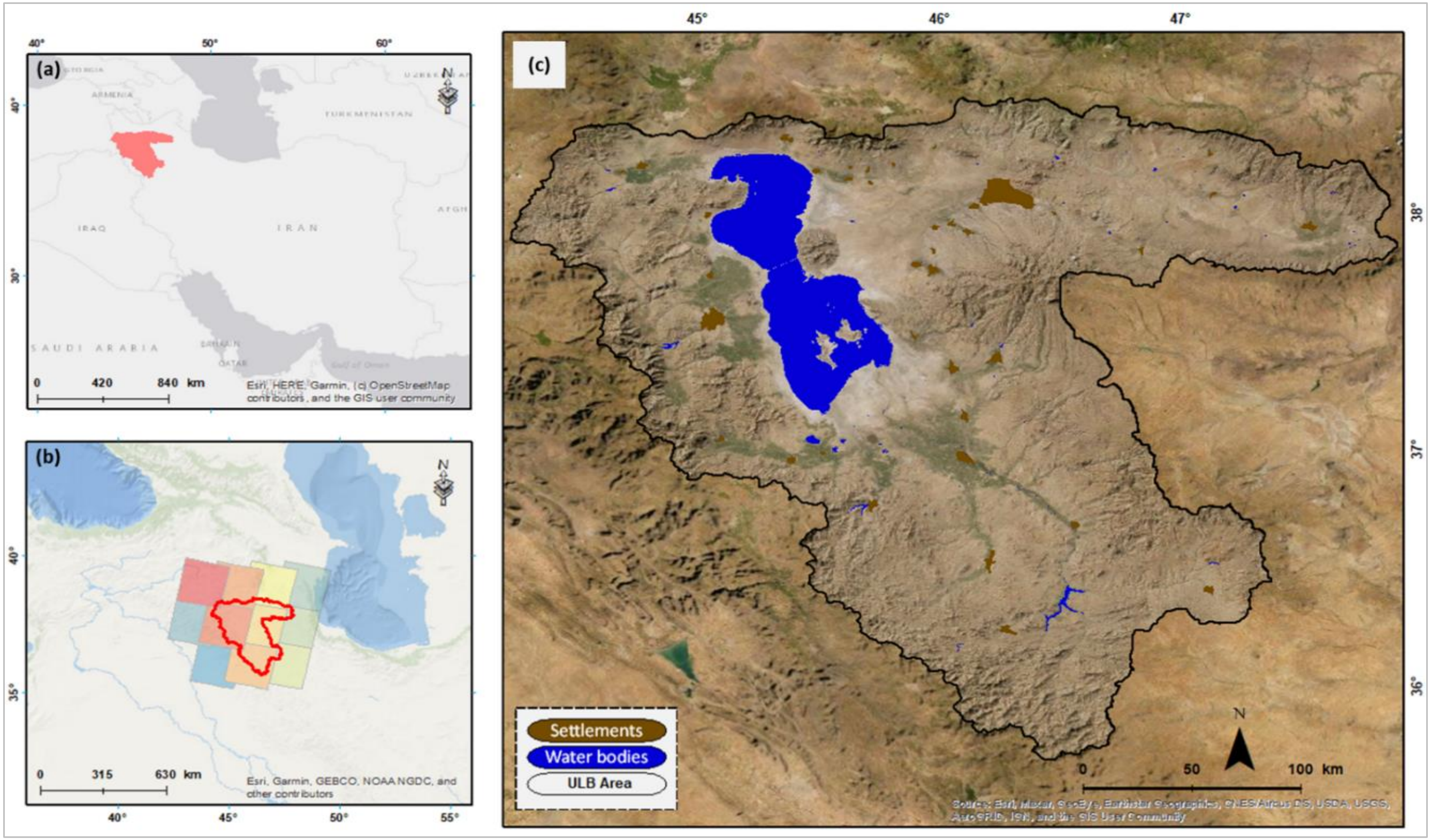

Play

Climate change impacts on the lake drought

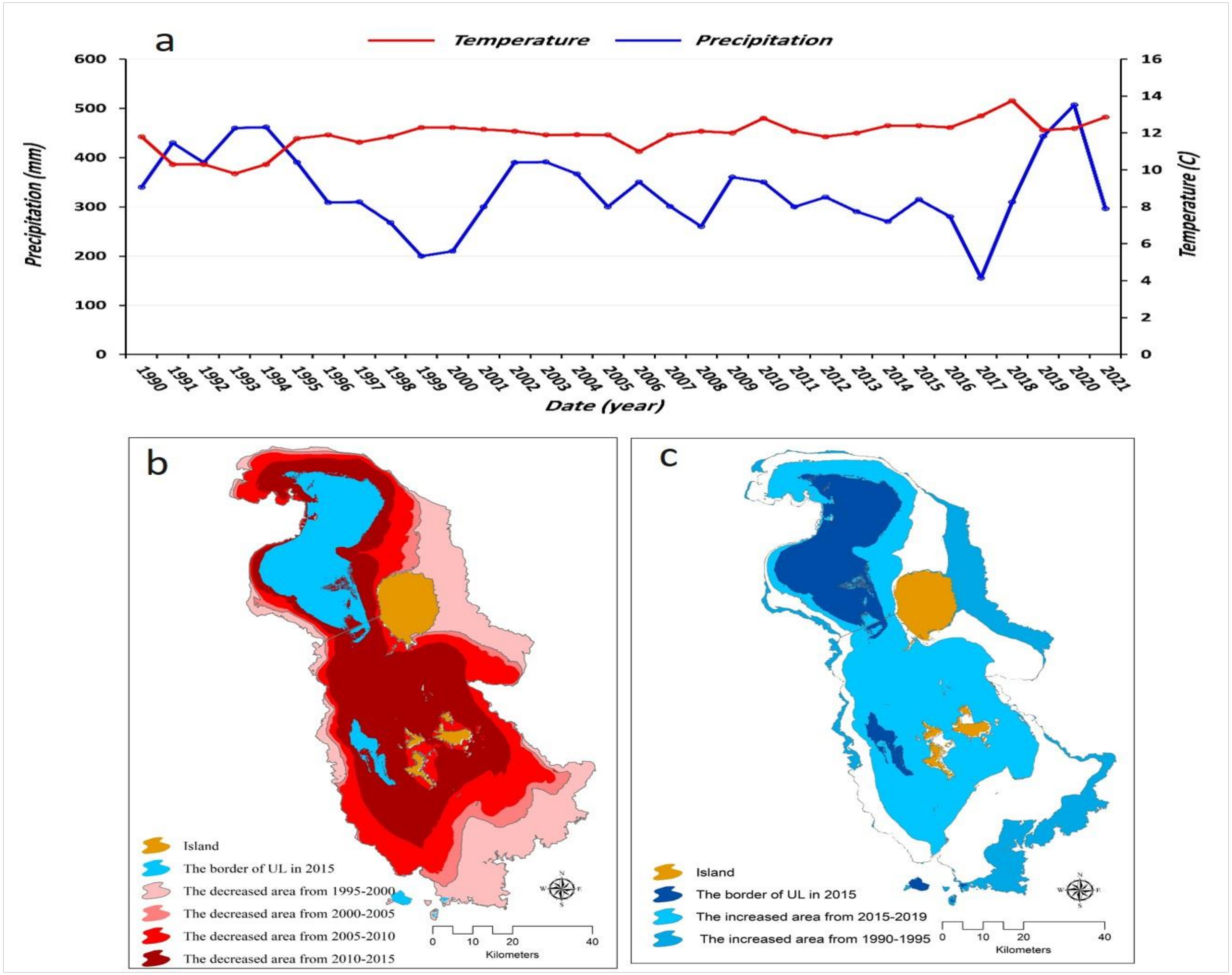

Environmental issues resulted by the lake drought

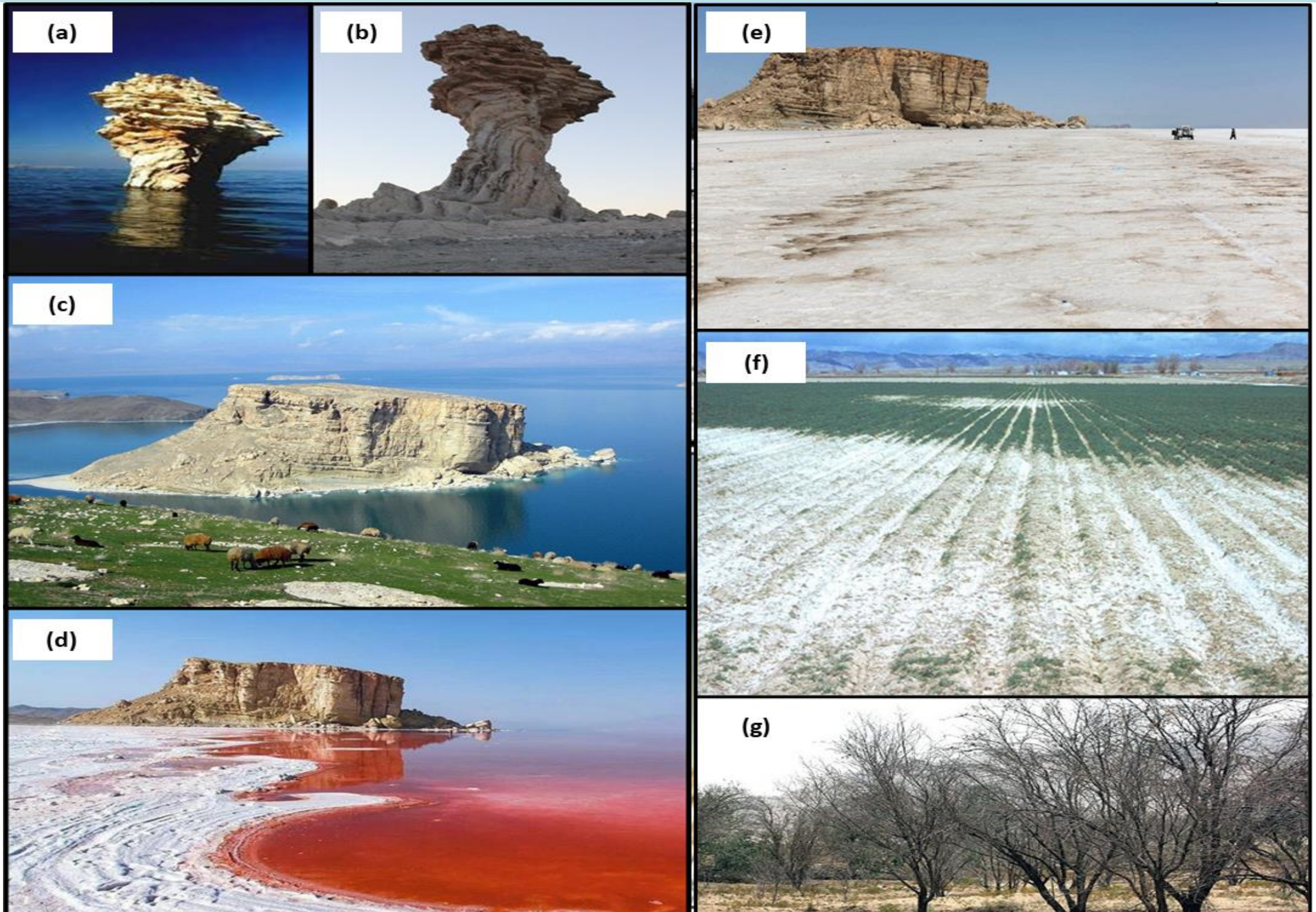

Salt-dust storms around the lake threats the productivity of farmlands and public health of the 7.3 million local inhibition

Time series land use/cover mapping and change detection based on different data driven approaches (1990-2020)

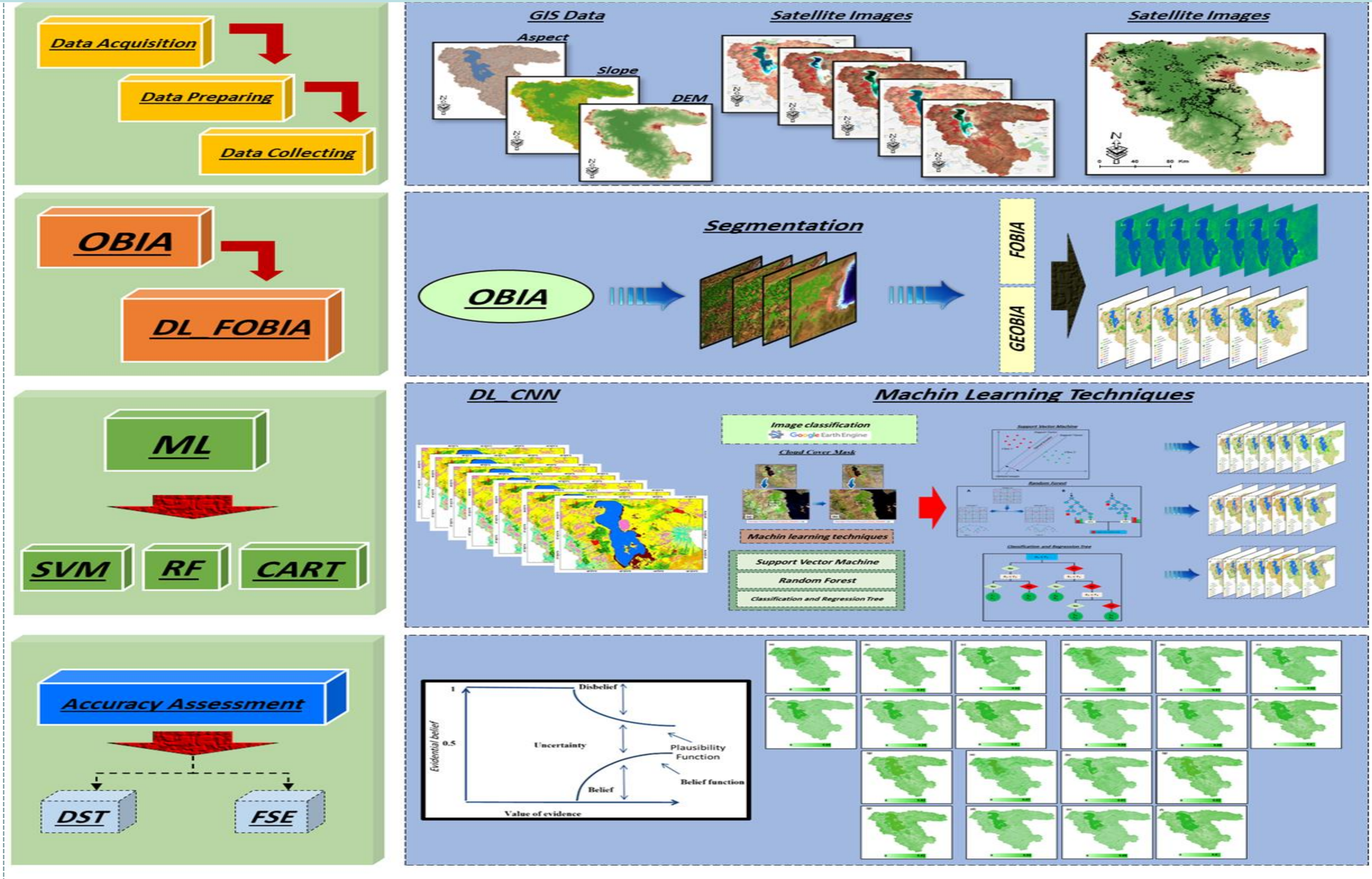

An integrated Fuzzy Object Based Image Analysis and Deep learning methods

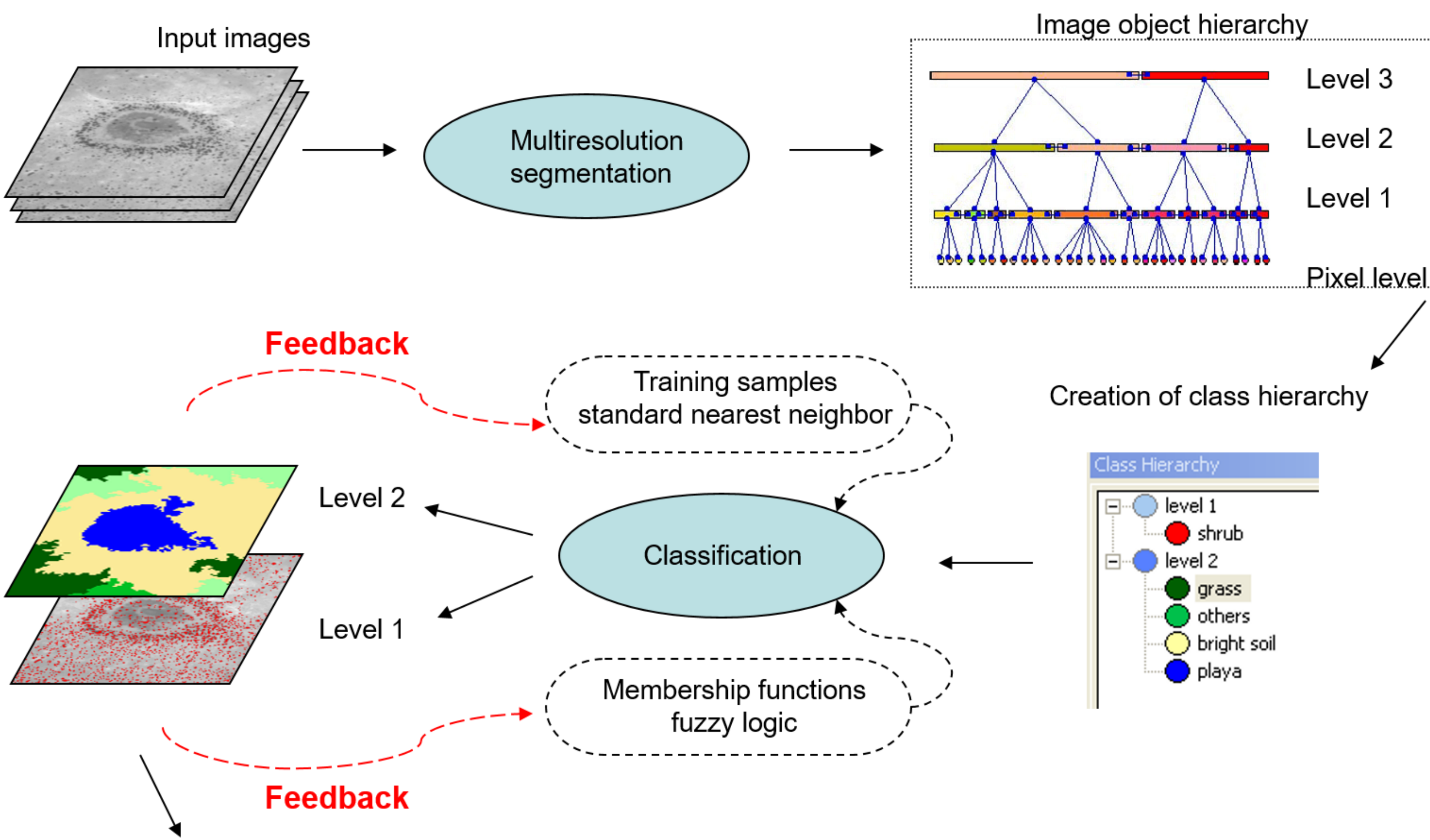

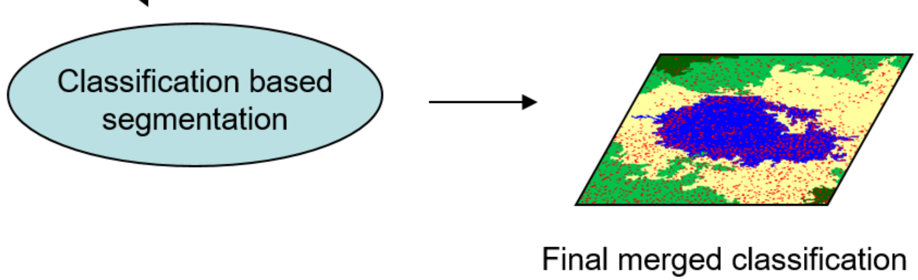

Segmentation parameters used for the analysis

Segmentation level	Scale	Color	Shape	Shape settings	
				Smoothness	Compactness
Level 1	3	0.8	0.2	0.8	0.2
Level 2	250	0.8	0.2	0.5	0.5

Scale is a unitless parameter related to the image resolution. Values for color and shape as well as smoothness and compactness are weighting factors ranging from 0 to 1.

Object based image analysis in integration with deep learning techniques for LULC mapping

Process related operation
- execute child processes
- set rule set options

Segmentation
- chessboard segmentation
- quadtree based segmentation
- contrast split segmentation
- multiresolution segmentation
- spectral difference segmentation
- contrast filter segmentation

Basic Classification
- assign class
- classification
- hierarchical classification
- remove classification

Advanced Classification
- find domain extrema
- find local extrema
- find enclosed by class
- find enclosed by image object
- connector
- optimal box

Variables operation
- update variable
- compute statistical value
- compose text
- apply parameter set
- update parameter set
- load parameter set
- save parameter set
- delete parameter set file
- load calibration parameter
- save calibration parameter
- add calibration parameter
- show open parameter set dialog

Reshaping
- remove objects
- shape split (prototype)
- merge region
- grow region
- multiresolution segmentation region
- image object fusion
- convert to sub-objects
- border optimization
- morphology
- watershed transformation

Level operation
- copy image object level
- delete image object level
- rename image object level

Interactive operations
- show user warning
- create/modify project (prototype)
- update action from parameter set
- update parameter set from action
- manual classification
- send windows command
- configure object table
- display image object level
- select input mode
- activate draw polygons
- select thematic objects
- end thematic edit mode

Sample operation
- classified image objects to samples
- cleanup redundant samples
- nearest neighbour configuration
- delete all samples
- delete samples of classes
- disconnect all samples
- sample selection

Image layer operation
- create temporary image layer
- delete image layer
- convolution filter
- layer normalization
- median filter
- pixel freq. filter
- edge extraction lee sigma
- edge extraction canny
- surface calculation
- layer arithmetics
- line extraction

Thematic layer operation
- synchronize image object hierarchy
- read thematic attribute
- write thematic attributes

Export
- export classification view
- export current view
- export thematic raster files
- export domain statistics
- export project statistics
- export object statistics
- export object statistics for report
- export vector layers
- export image object view

Workspace automation
- create scene copy
- create scene subset
- create scene tiles
- submit scenes for analysis
- delete scenes
- read subscene statistics

Implementation of different OBIA's features for LULC classification

	Quantifiable attribute	Mathematical formulation
Spectral attributes	Brightness	$B = \frac{1}{n_{vis}} \sum_{i=1}^{n_{vis}} \bar{c}_{i(vis)}$ B is the mean brightness of an object and $\bar{C}_{i(vis)}$ is the sum of all the mean brightnesses in the visible bands divided by the corresponding number of bands n_{vis}
	Normalized Difference Vegetation Index (NDVI)	Tv = mean NDVI $f\,(\text{Object}) = \begin{cases} LC \text{ if } f(\text{Object}) \leq T_v) \\ VA \text{ if } f(\text{Object}) > T_v) \end{cases}$ $T'_v = \frac{\text{meanNDVI}_{LC}+\text{meanNDVI}_{VA}}{2}$ T'_v is an average of the mean NDVI values for "landslide candidates" (LC) and vegetated areas (VA). The NDVI, which has a value between −1.0 and +1.0
	Specific leaf area vegetation index (SLAVI)	SLAVI = 100*[Mean band 4]/([Mean band 3]+[Mean band 5])
	Green Normalized Difference Vegetation Index (GNDVI)	GNDVI = 100*(1+(([Mean band 4]-[Mean band 2])/([Mean band 4]+[Mean Layer 2]))
	Modified Normalized Differenced Water Index (MNDWI)	MNDWI = 100*(1+(([Mean Band4]-[Mean Band5])/([Mean Band4] +[Mean Band5]))
	Normalized Built-up Index (NDBI)	NDBI = ([Mean band 5]-[Mean band 4])/([Mean band 5]+[Mean band 4])
	Soil Water Content Index (InfraRed Index)	SWCI (IR) = (NIR – ETM7)/ (NIR+ETM7)
	Soil Color Index	SCI = R – G/R +G
	Normalized Built-up Index (NDBI)	NDBI = ([Mean band 5]-[Mean band 4])/([Mean band 5]+[Mean band 4])
	Salinity Index (SI)	Salinity Index (SI) = ([Mean Layer 1]*[Mean Layer 3])^0.5
	Normalized Difference Salinity Index	NDSI = ([Mean band 3]-[Mean band 4])/([Mean band 3]+[Mean band 4])
	mean band	$\bar{C}_k(V) = \bar{C}_k(P_v) = \frac{1}{\#P_v} \sum_{(x,y,z,t)\in P_v} \bar{C}_k(x,y,z,t)[C_k^{min}, C_k^{max}]$
	Standard Deviation	$\sigma_k(v) = \sigma_k(P_v)\sqrt{\frac{1}{\#P_v}\left(\sum_{(x,y,z,t)\varepsilon P_v} C_k^2(x,y,z,t) - \frac{1}{\#P_v}\left(\sum_{(x,y,z,t)\varepsilon P_v} C_k^2(x,y,z,t)\right)^2\right)}\,[0, \tfrac{1}{2}C_k^{range}]$ • $\sigma_k(v)$ is the standard deviation of intensity values of image layer k of all pixel/voxels forming an image object v • Pv is the set of pixel/voxels of an image object v • #Pv is the total number of pixel/voxels contained in Pv • (x,y, z, t) are the pixel/voxel co-ordinates • c_k(x,y, z, t) is the image layer intensity value at pixel/voxel (x,y, z, t) • C_k^{range} is the data range of image layer k with $C_k^{range} = C_k^{max}$]-C_k^{min}
Geometric attributes	Shape length/width	$\frac{\text{Length}}{\text{Width}}$ Length of the image object Width of the image object
	Shape asymmetry	$1 - \sqrt{\frac{\lambda_{min}}{\lambda_{max}}}$ λ_{min} is the minimal eigenvalue
	Shape Rectangular	λ_{max} is the maximal eigenvalue $\frac{\{\#(x,y)\varepsilon P_v : \rho v(x,y\rho) \leq 1\}}{\#P_v}$ P_v = (x,y) is the elliptic distance at a pixel (x,y) [0,1]; where 1 is a perfect rectangle.
	Shape Index	$\frac{B_v}{4\sqrt{\#v_v}}$ B_v is the image object border length

Implementation of different OBIA’s features for LULC classification

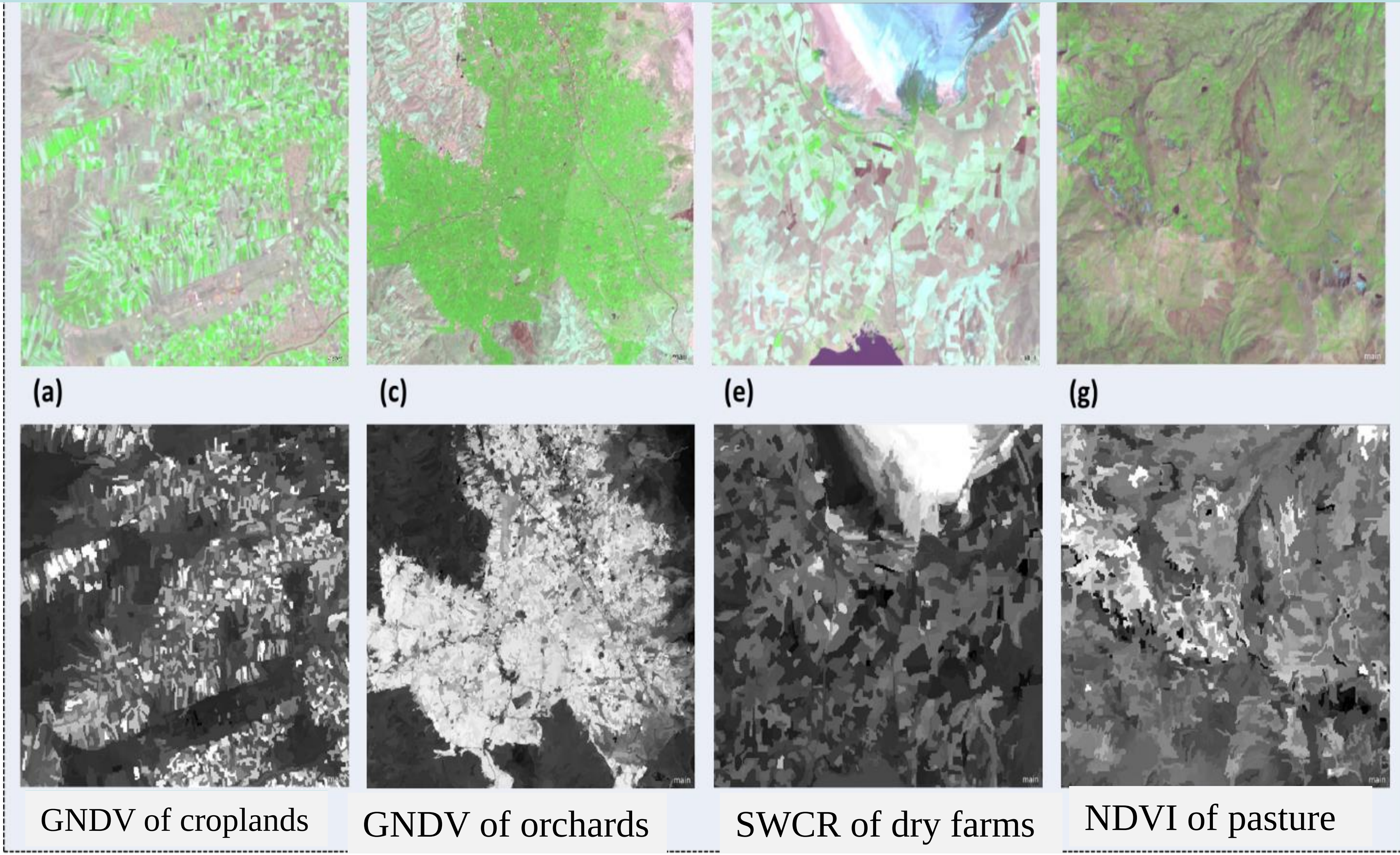

Satellite image and resulting object-features for a selected area in ULB, namely: a) croplands, b) GNDV of croplands, c) Orchards, d) GNDVI of croplands, e) dry farms; f) SWCR of dry farms; pasture and rangelands; h) NDVI of pasture and rangelands

LULC classes and their respective thresholds obtained for object features

	-0.123<Mean NDVI<0.365
Rock output	TRI≥5 0≤Relief≤110 NDVI<0.05
Dry and fallow lands	0<Mean NDVI<0.1 0≤SWCI (IR)≤0.4 1.02≤Shape Index≤1.36 Rectangular fit≥0.84 2.5531 <GLCM Contrast<9.642 SCI≤0.04
Pasture lands	Mean Slope ≥ 5 Mean NDVI≥0.18
Rangelands	Mean Slope ≥ 5 Mean NDVI≥0.08

Results of the LULC classification based on the FOBIA-DL
a) ۱۹۹۰, b) ۱۹۹۵, c) 20۰۰, d) 2005, e) 20۱0, f) ۲۰۱۵ and g) ۲۰۲۰

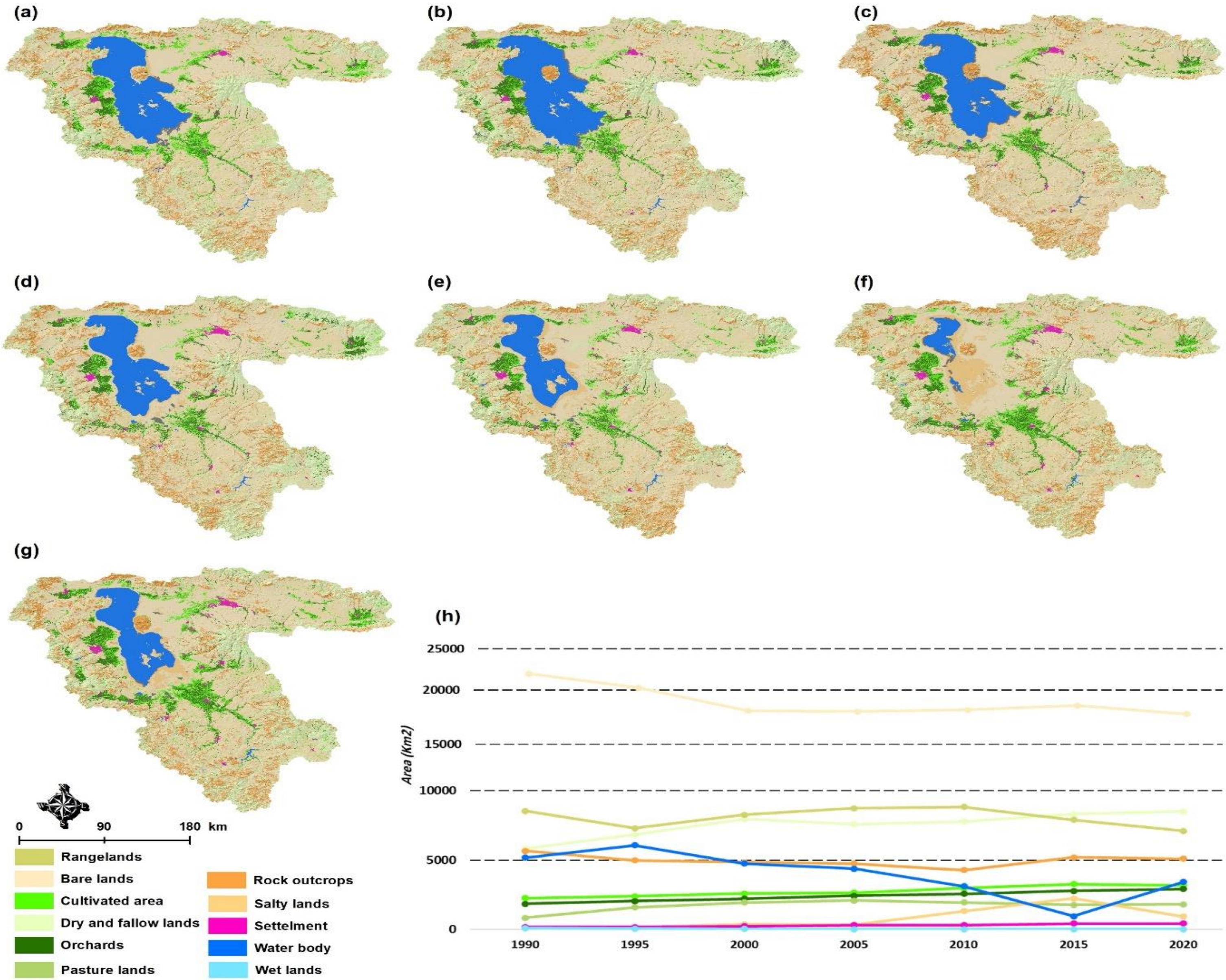

Difference function and its respective default values for each category

Confidence in classification	Very High Confidence in Classification (VHCC)	*		≥ 90
	High Confidence in Classification (HCC)	*		≥ 85
	Acceptable Confidence in Classification (ACC)		*	≥ 80
	Reduced Confidence in Classification (RCC)	*		80 ≤
	Very Reduced Confidence in Classification (VRCC)		*	50
	Acceptable Error (AE)			50 ≤
Magnitude errors	High Error (HE)			≥ 85
	Very High Error (VHE)			≥ 90

Journals & Magazines > IEEE Geoscience and Remote Se... > Volume: 15 Issue: 1

A Novel Approach of Fuzzy Dempster–Shafer Theory for Spatial Uncertainty Analysis and Accuracy Assessment of Object-Based Image Classification

Publisher: IEEE

Cite This PDF

Dempster-Shafer Theory for spatial accuracy assessment

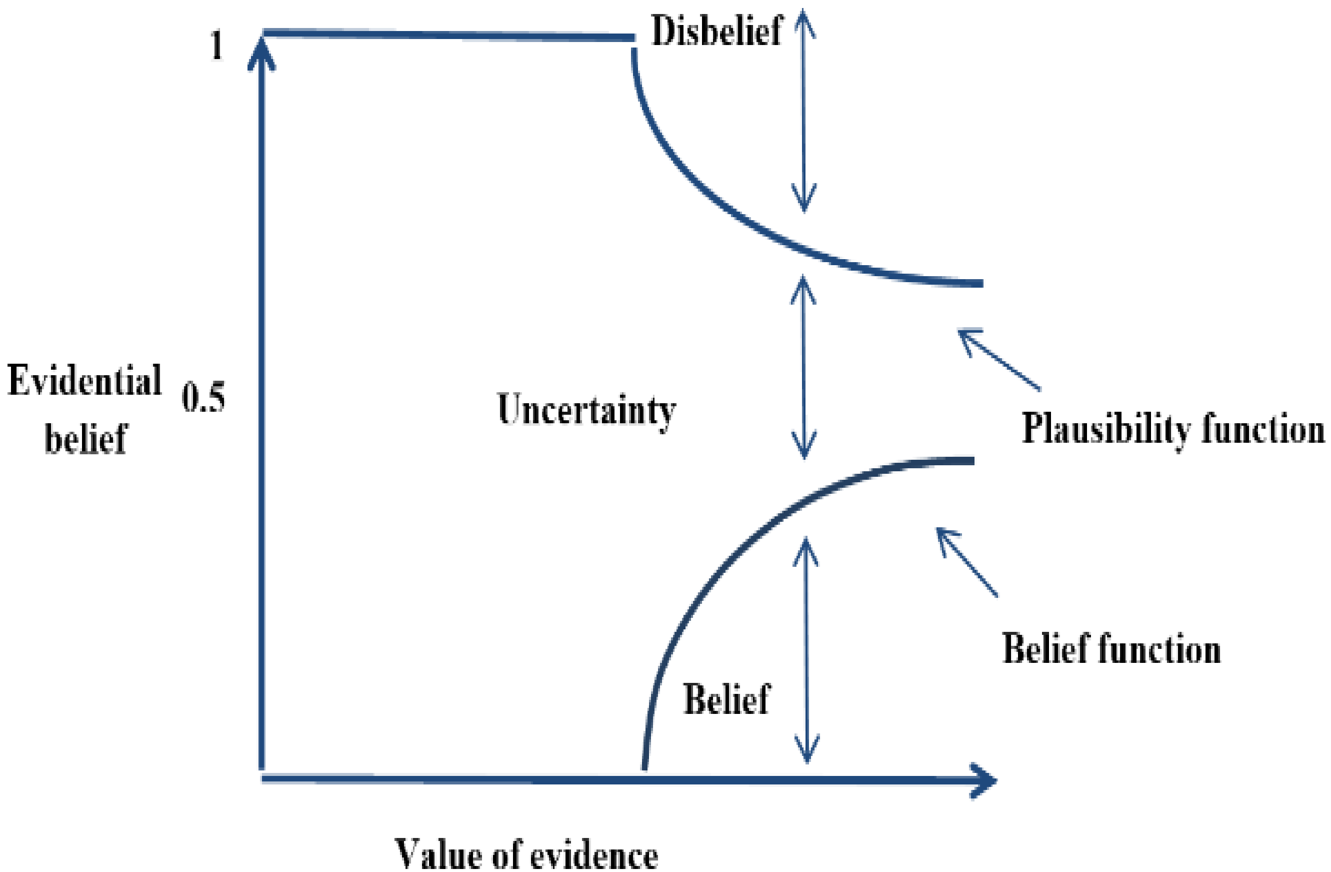

Results of the spatial uncertainty analysis for the FOBIA-DL

a) 2020, b) 2015, c) 2010, d) 2005, e) 2000, f) 1995 and g) 1990

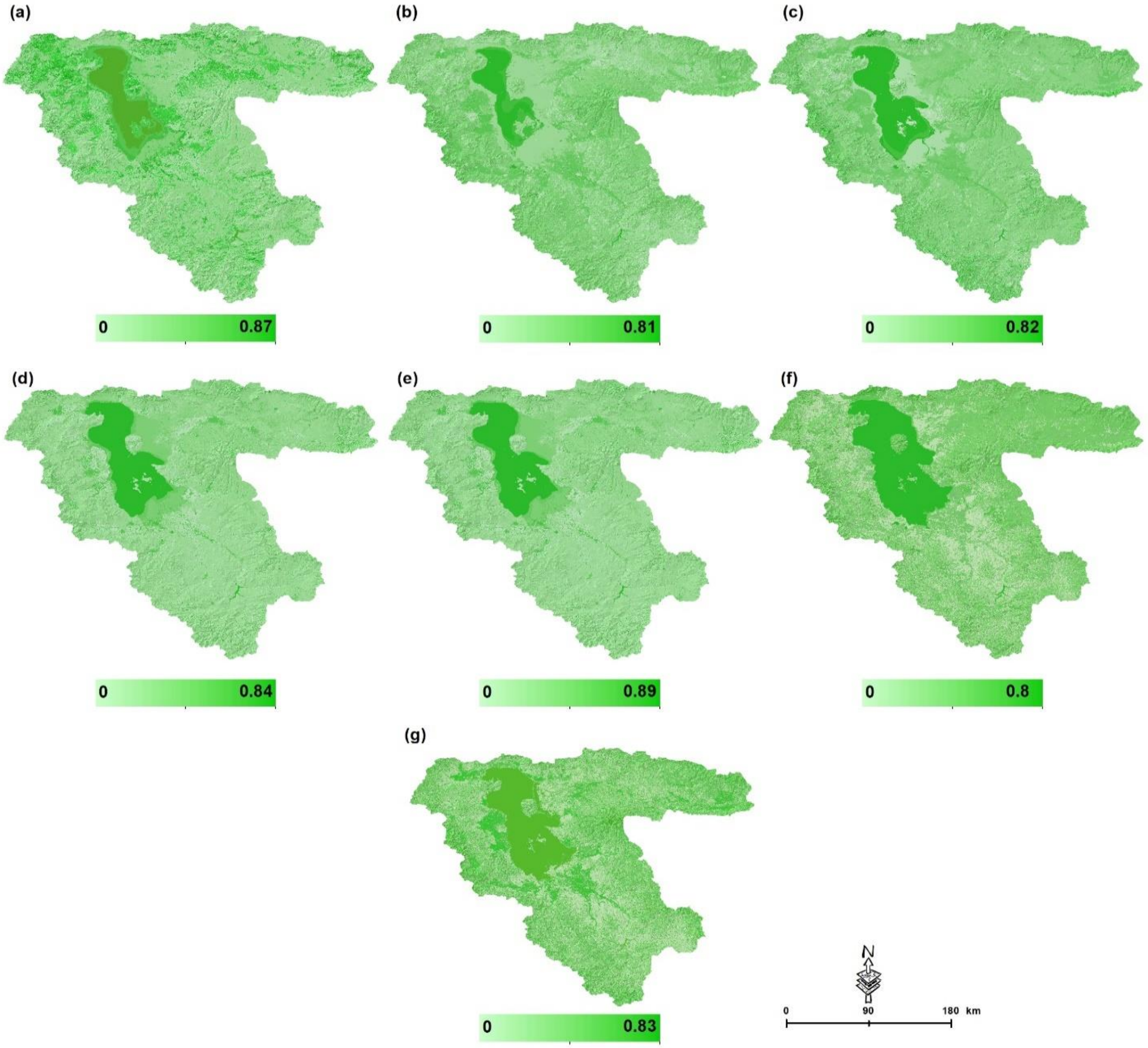

Comparing efficiency of machine learning data-driven approaches for land use/cover mapping and trend analysis using Google Earth Engine: Support Vector Machine (SVM), Random Forest (RF) and Classification and Regression Tree (CART).

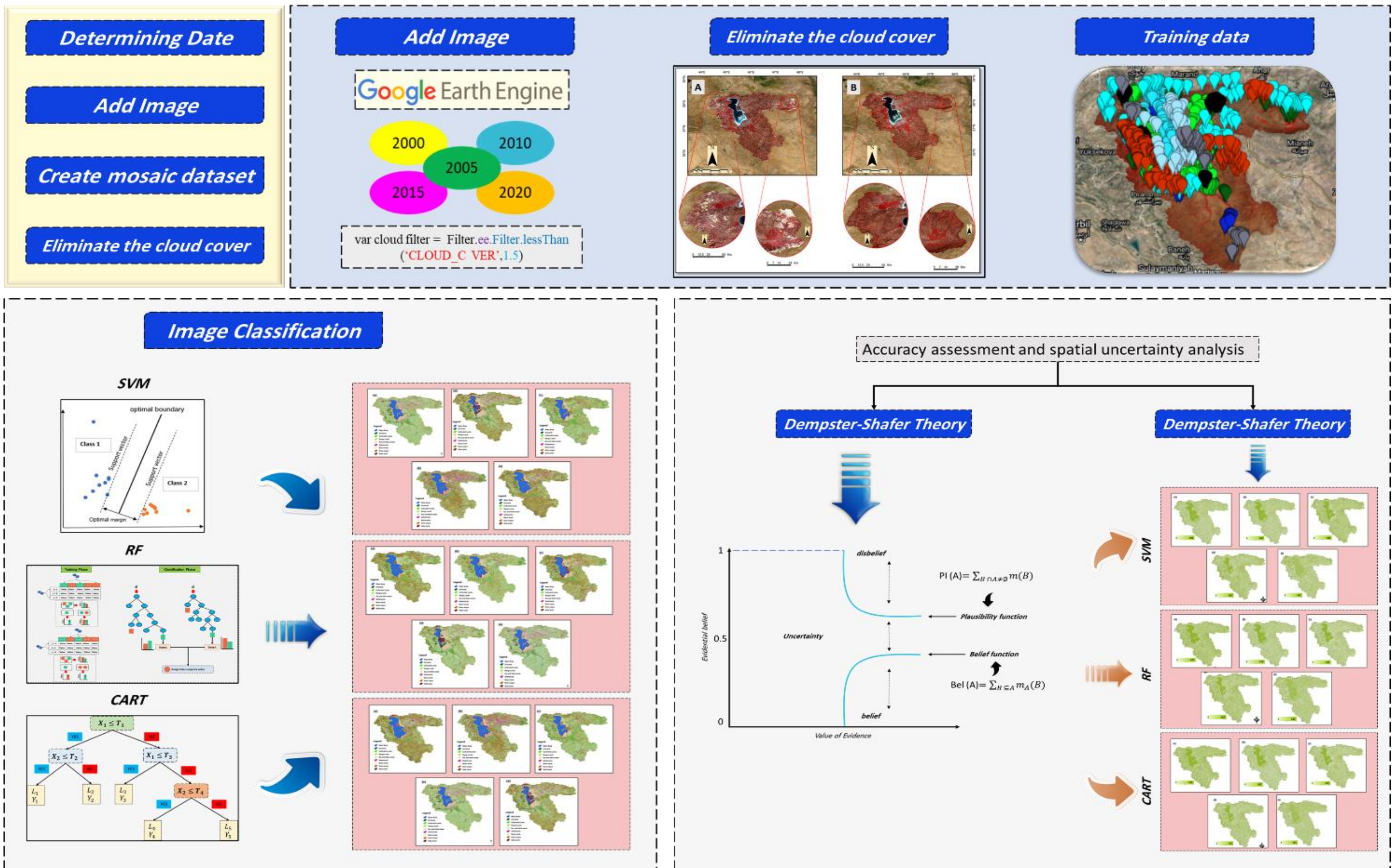

Comparing efficiency of different data driven approach

Table 5. Results of the accuracy assessment and ICR values for the FOBIA-DL based classified LULC maps

Method	1990	1995	2000	2005	2010	2015	2020
FOBIA-DL	0.94	0.93	0.98	0.95	0.96	0.93	0.97
SVM	0.83	0.80	0.89	0.84	0.82	0.81	0.87
RF	0.72	0.73	0.75	0.78	0.79	0.77	0.76
CART	0.62	0.63	0.64	0.65	0.68	0.67	0.66

VRCC	0.05	0.10	0.02	0.05	0.05	0.08	0.02	0.09	0.08	0.06	0.05	0.04	0.06	0.05	0.07	0.04	0.05	0.02	0.04	0.09	0.02
AE	0.01	0.02	0.03	0.02	0.03	0.01	00.2	0.03	0.01	0.02	0.03	0.02	0.02	0.02	0.03	0.02	0.01	0.02	0.03	0.02	0.01
HE	0	0	0	0	0	0	0	0	0	0	0	0	0	0	0	0	0	0	0	0	0
CHE	0	0	0	0	0	0	0	0	0	0	0	0	0	0	0	0	0	0	0	0	0
FSE %	92.2	90.1	91.4	94.6	92.1	91.4	93.6	92.4	93.1	95.1	96.2	94.2	96.1	95.6	94.1	93.3	92.8	91.9	93.2	91.6	95.2

Spatiotemporal soil salinization mapping under impacts of lake drought

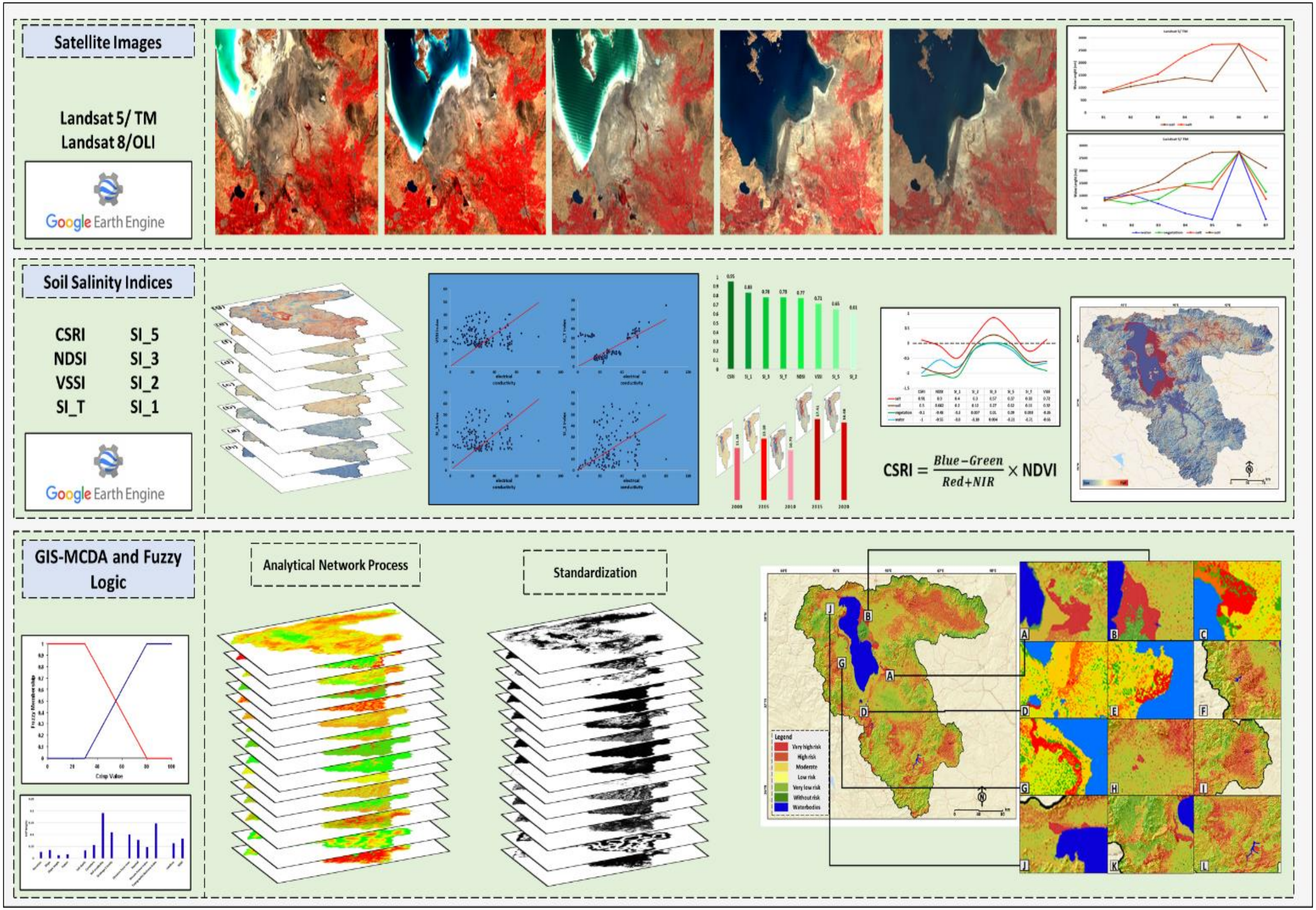

Deep learning convolutional neural network for soil salinization mapping

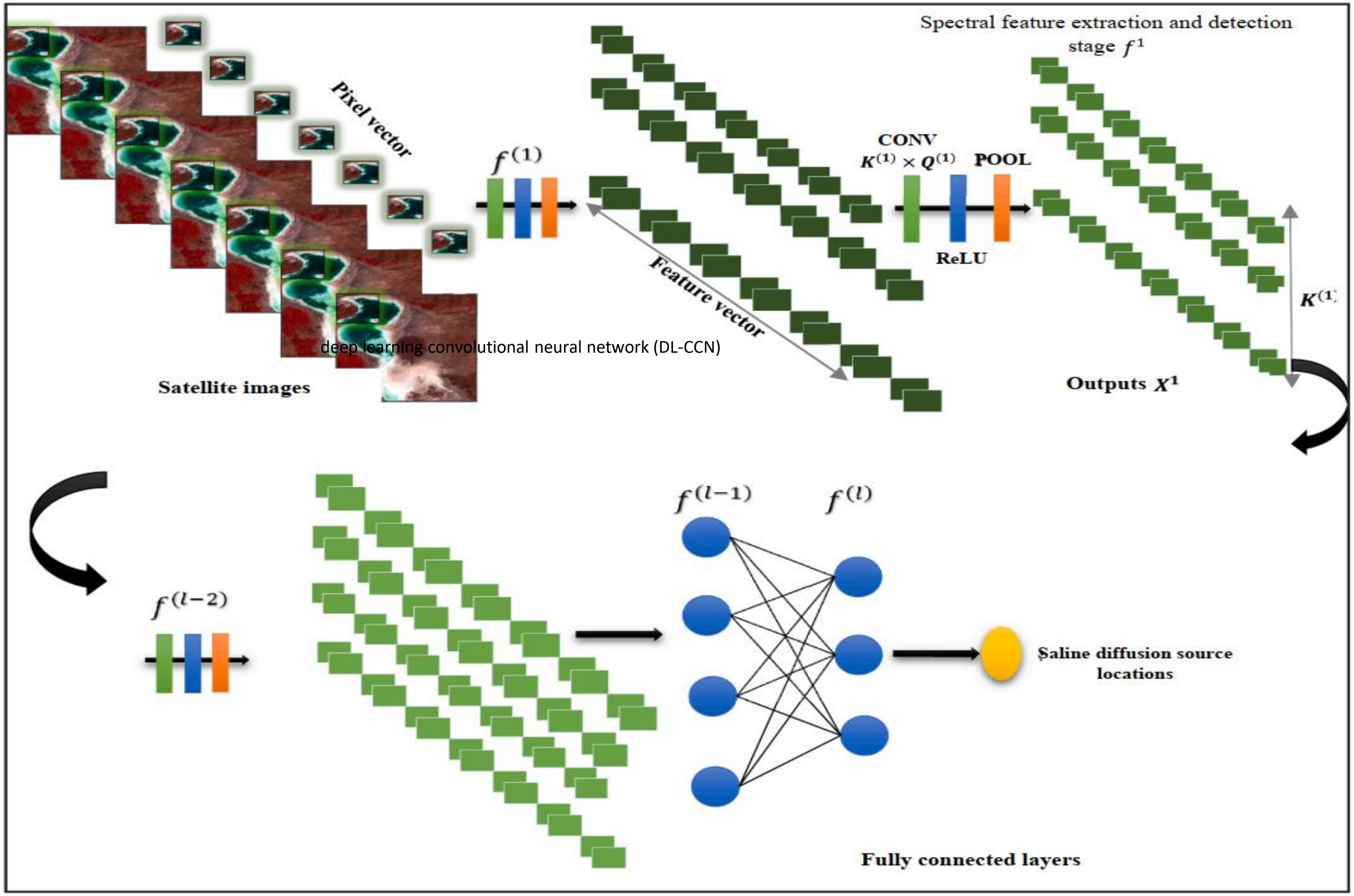

Soil Salinity Indices

index	Equation	Reference
Combined Spectral Response Index	(B+G)/(R+NIR) × NDVI	Fernandez-Buces et al, 2006
Normalized Differential Salinity Index (NDSI)	(R-NIR)/(R+NIR)	Khan et al, 2001
Salinity index (SI-T)	(R / NIR) × 100	Tripathi et al, 1997
Salinity Index (SI-1)	NIR/SWIR	Bannari et al, 2008
Salinity Index (SI-2)	(B-R)/(B+R)	Khan and Abbas, 2007
Salinity Index (SI-3)	(B×R)/G	Khan and Abbas, 2007
Normalized Differential Infrared Index	(NIR-SWIR1)/(NIR+SWIR1)	Elhag and Bahrawi, 2017
Vegetation Soil Salinity Index (VSSI)	2 × G – 5 × (R + NIR)	Dehni and Lounis, 2012

The soil salinity indices (a) Combined Spectral Response Index (CSRI), (b) Normalized Differential Salinity Index (NDSI), (c) Vegetation Soil Salinity Index (VSSI), (d) SI-T, (e) SI-1, (f) SI-2, (g) SI-3 and, (h) Normalized Differential Infrared Index.

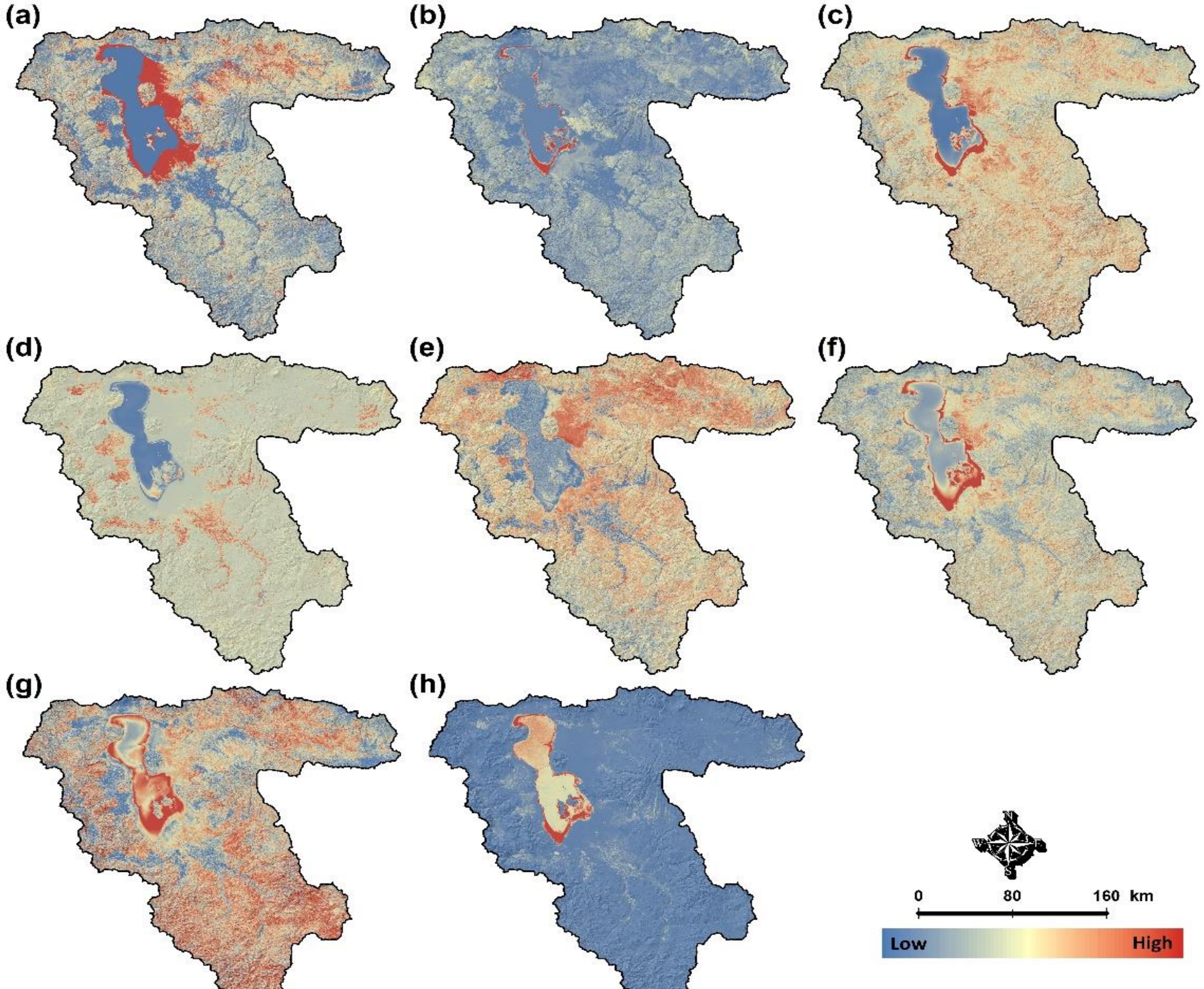

Correlation between indices values and field observation of soil salinity measurements; a) VSSI, b) SI_T, c) SI_5, d) SI_3, e) SI_2, f) SI_1, g) NDSI, h) CSRI and, k) accuracy of each index

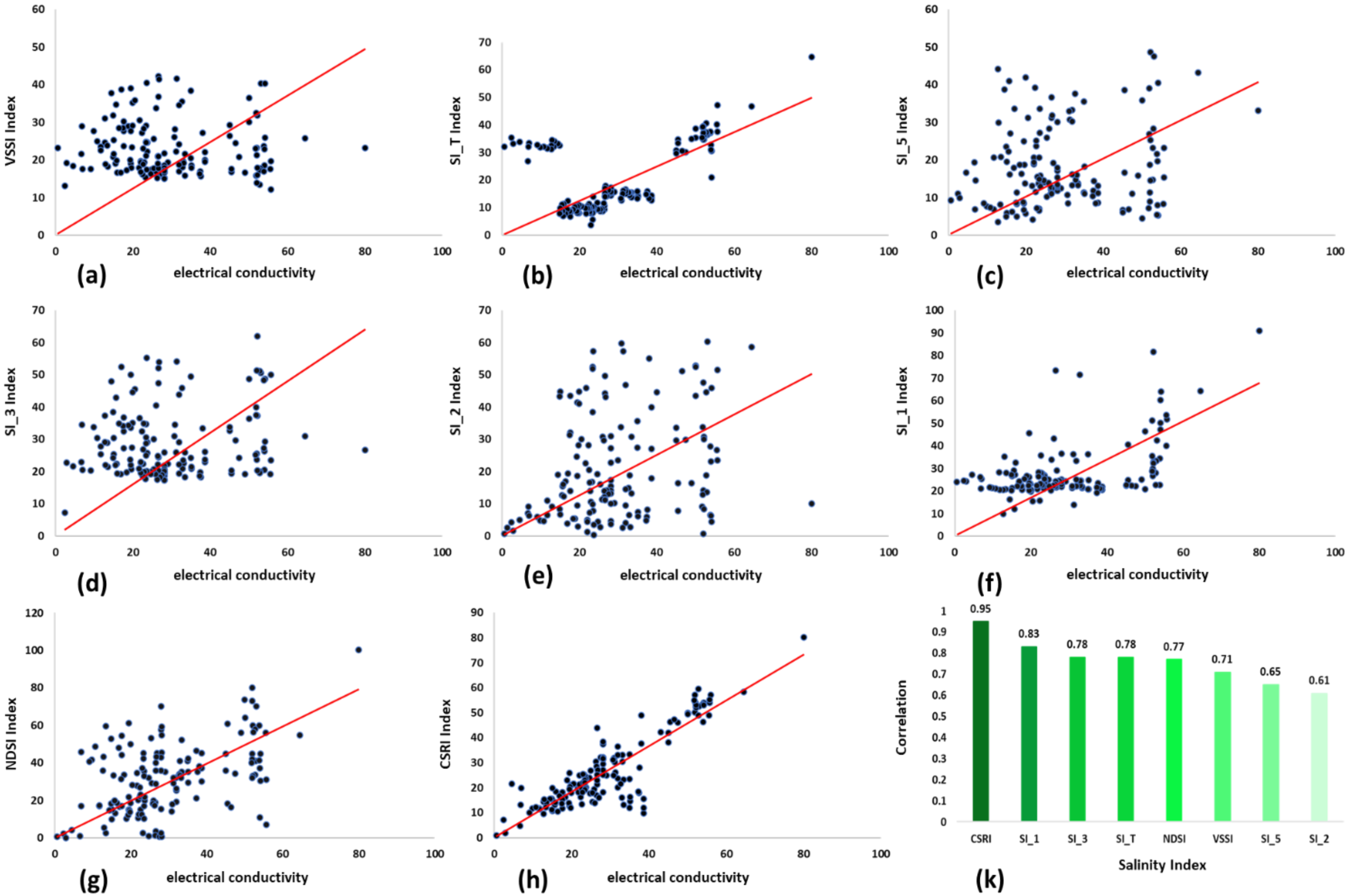

Soil salinity from 1990 to 2020 using Combined Spectral Response Index, a) 1990, b) 1995, c) 2000, d) 2005, e) 2010, f)2015, g)2020

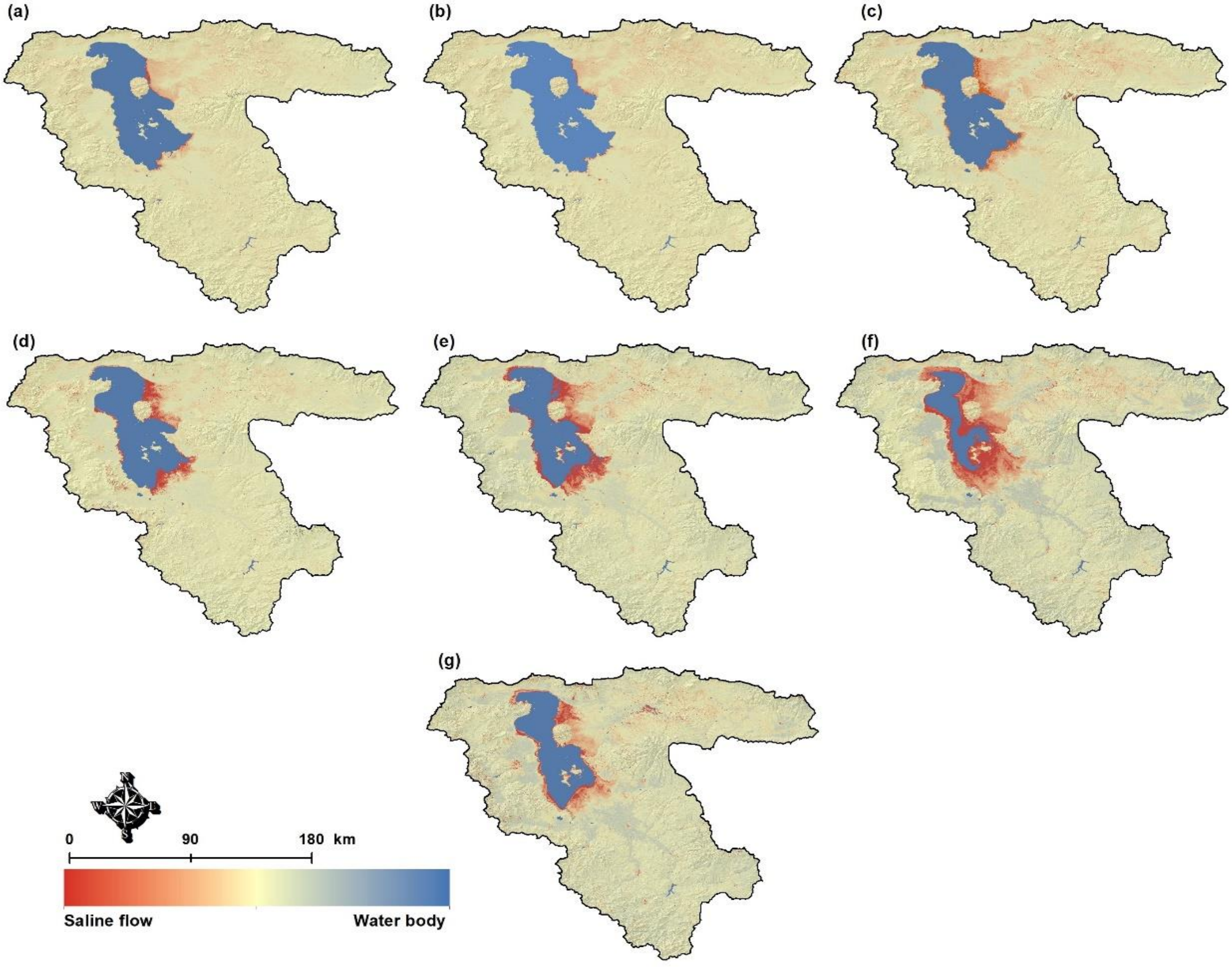

Extensive ongoing land subsidence due to the discharge of nearby aquifers around the lake

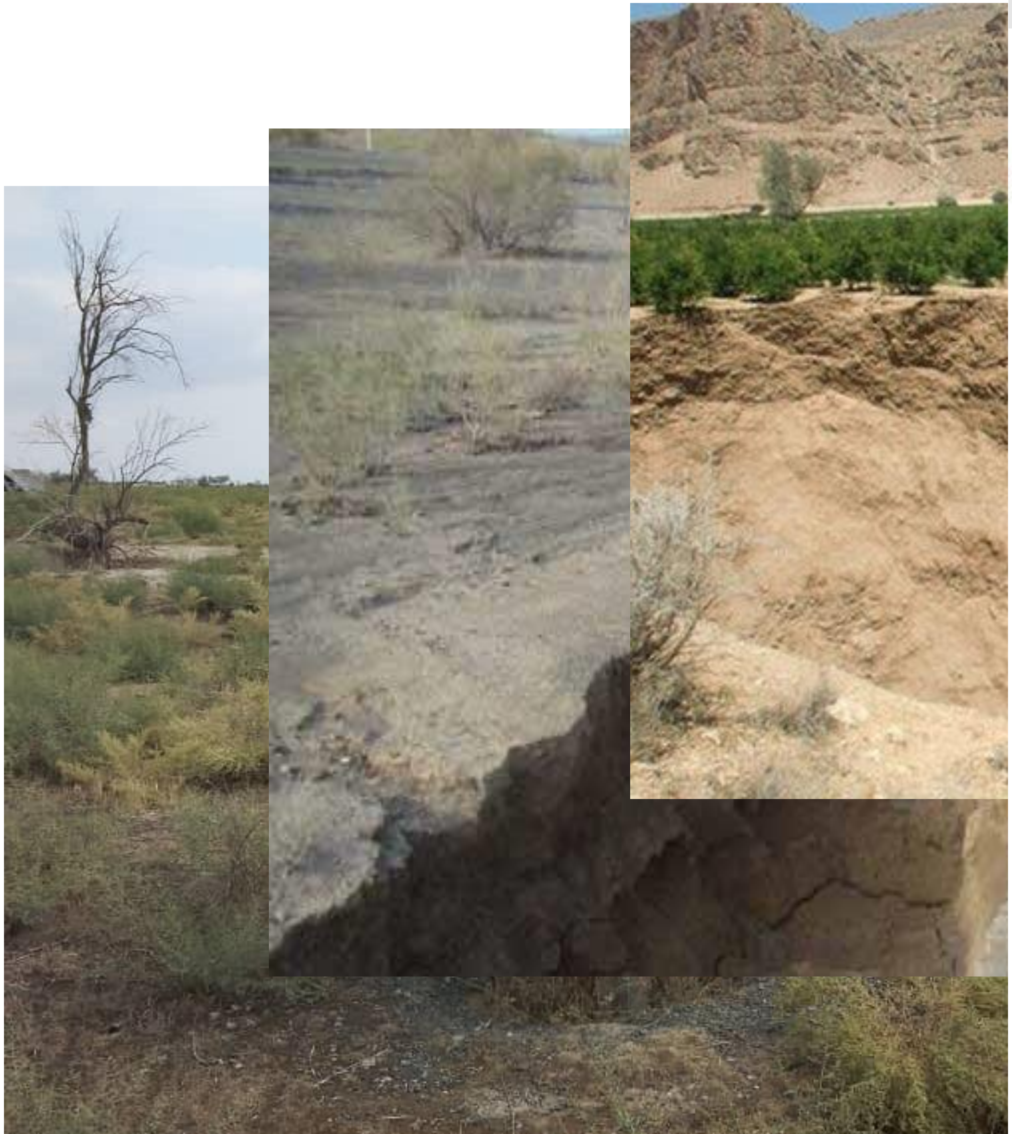

2015- 2020

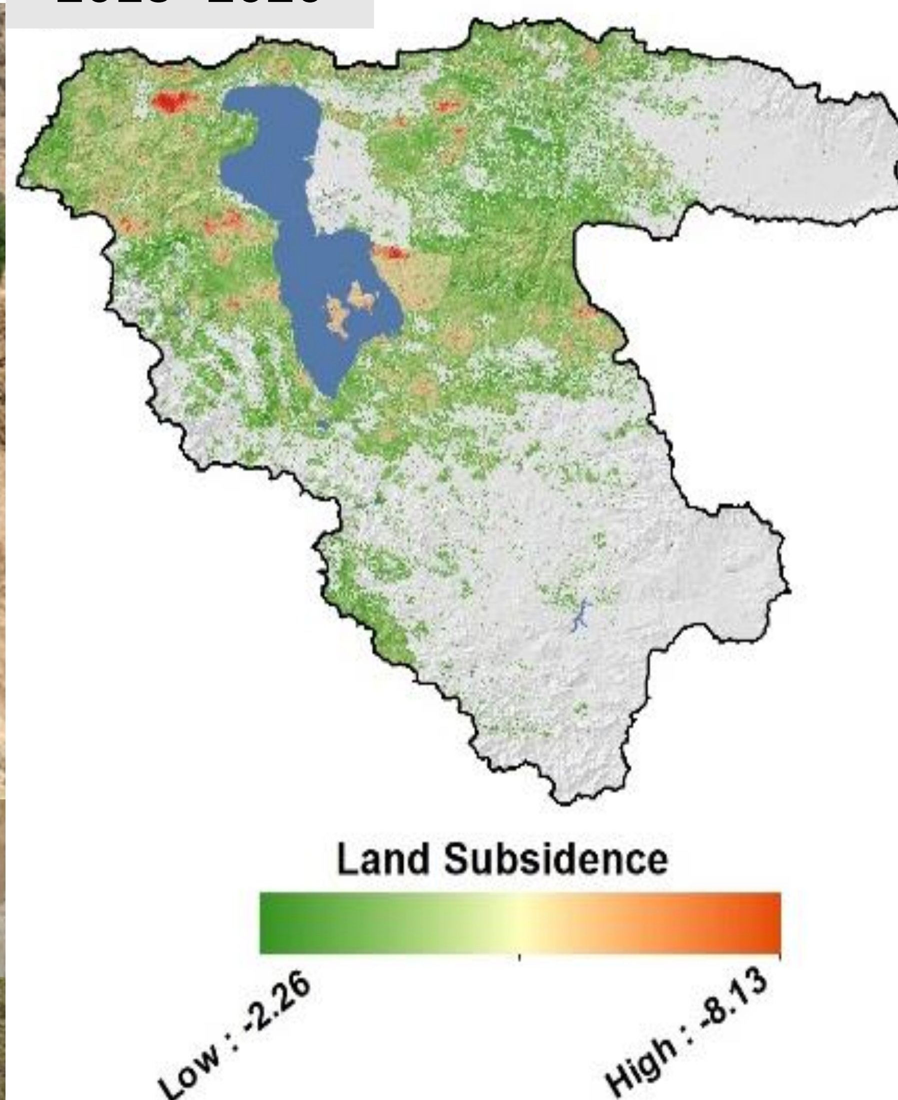

land degradation mapping

Criteria	Elements	FANP's Weights	*S*	*St*
Topography	Elevation	0.027	0.031	0.044
	Slope degree	0.035	0.071	0.071
	Slope length	0.013	0.008	0.004
	Aspect	0.016	0.008	0.028
	Curvature	0.056	0.126	0.218
Soil characteristics	Soil depth	0.033	0.010	0.072
	Soil texter	0.191	0.188	0.296
Hydrology	Distance from river	0.101	0.182	0.198
	Drainage density	0.102	0. 152	0.148
	Annual precipitation	0.077	0.015	0.161
	Stream Power Index	0.048	0.068	0.166
	Topographic Wetness Index	0.147	0.189	0.249
Anthropic	Land use	0.063	0.115	0.165
	Vegetation denticity	0.083	0.071	0.074

GIS spatial decision making systems applied to land degradation assessment

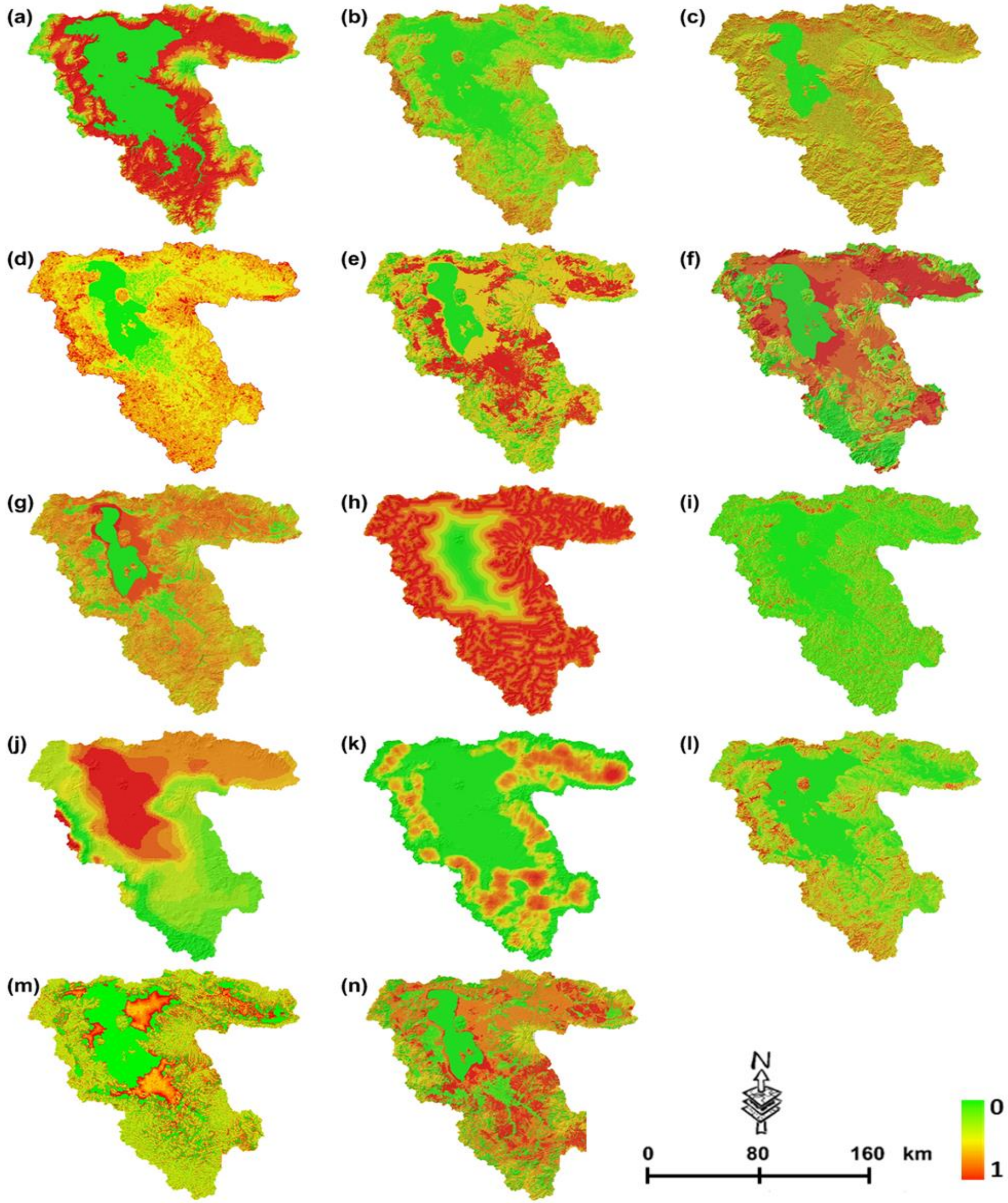

- a) Elevation
- b) Slope degree
- c) Slope aspect,
- d) Curvature
- e) Soil depth
- f) Soil erodibility
- g) NDVI
- h) Distance from rivers
- i) Stream Power Index
- j) Precipitation
- k) Drainage density
- l) Slope length
- m) Topographic wetness index
- n) LULC

GIS spatial decision making systems applied to land degradation assessment

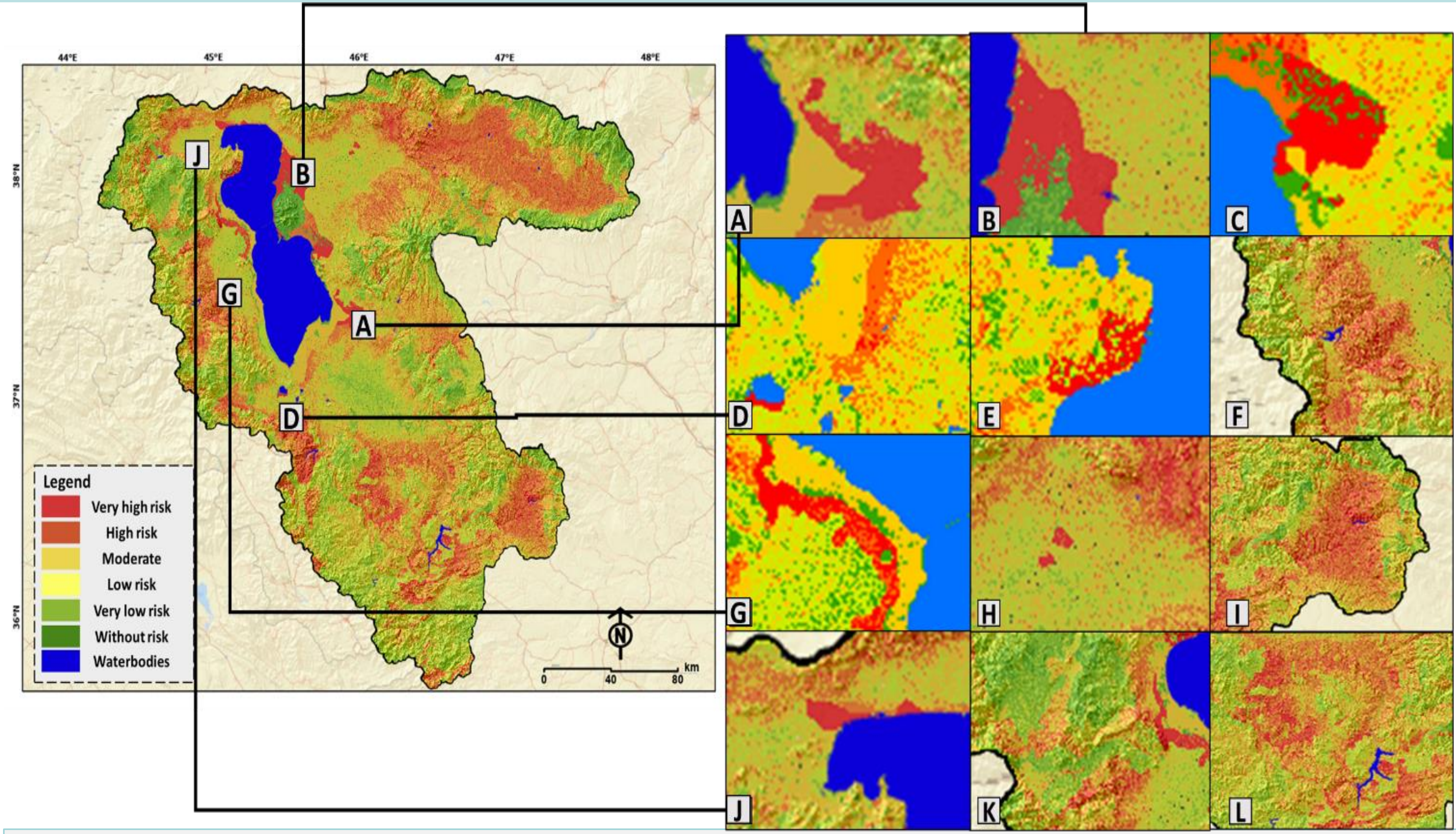

According to the final result, 12.49% of the area is affected by very high risk, 25.96% is at high risk, and the rest of the study area has moderate and lower than the moderate risk of soil erosion

Land use/cover change as main reason for lake drought (95000 wells around the lake)

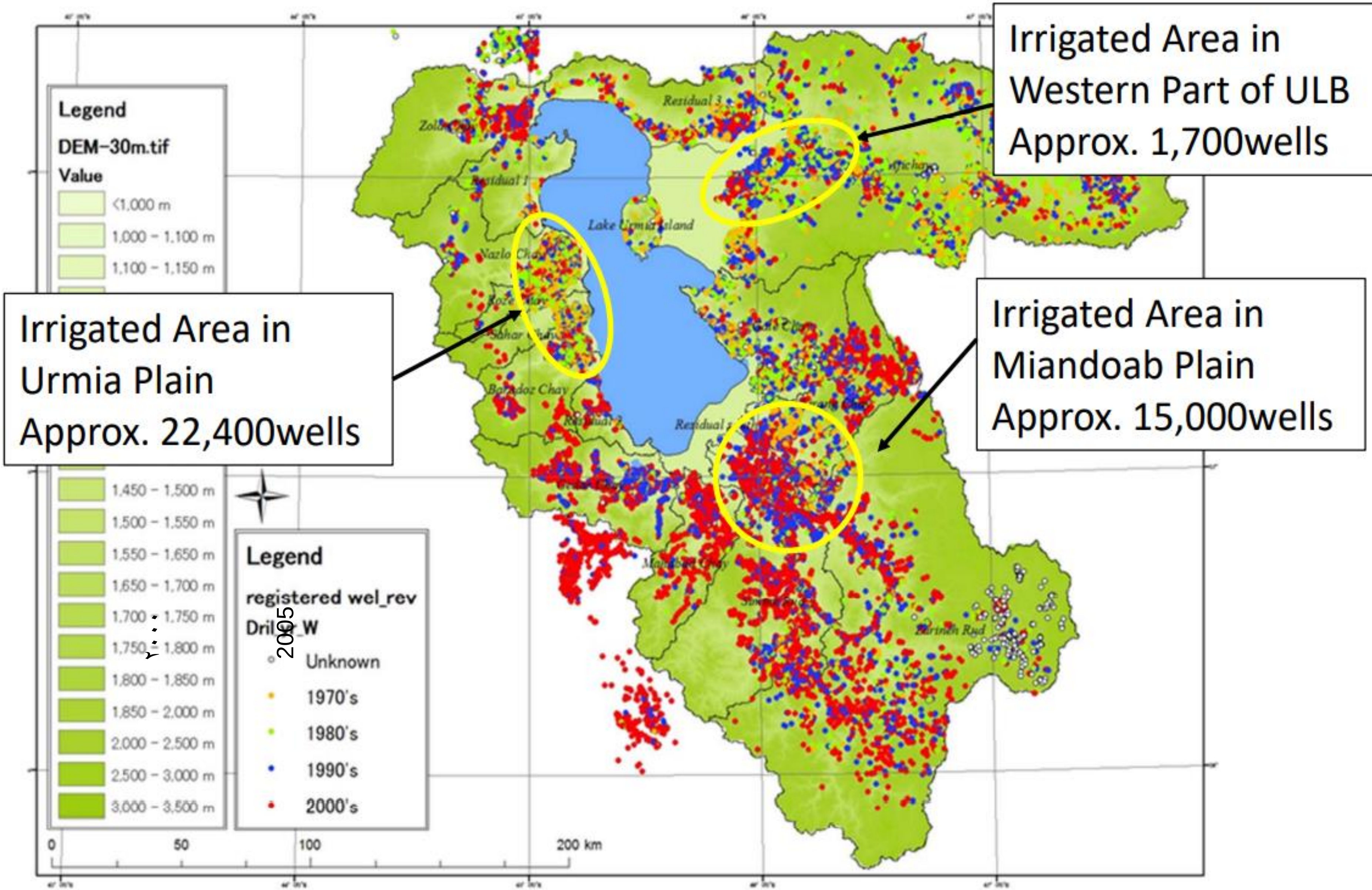

Trend analysis for extensive groundwater discharge

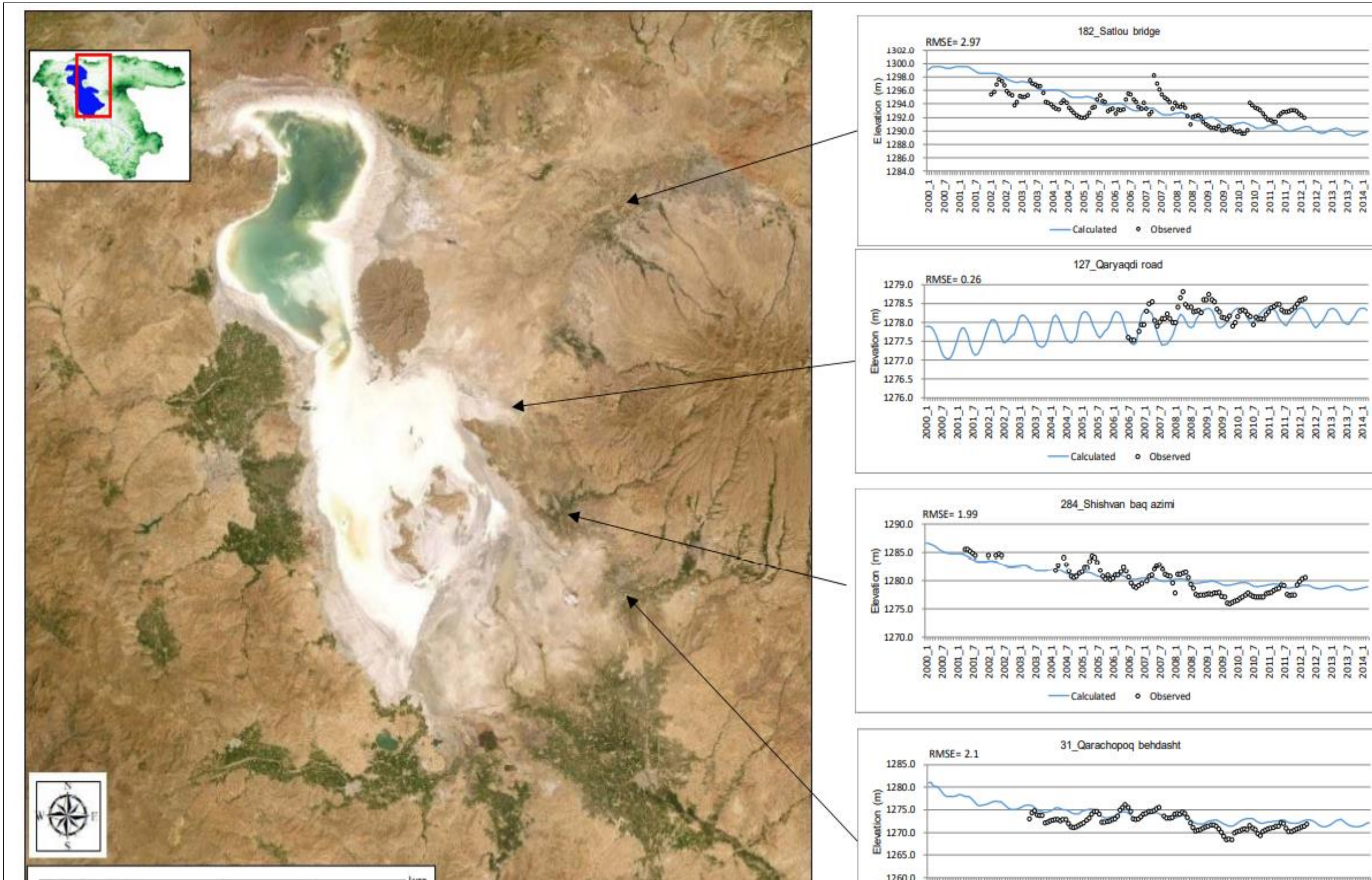

Saltwater Intrusion Problem Identification

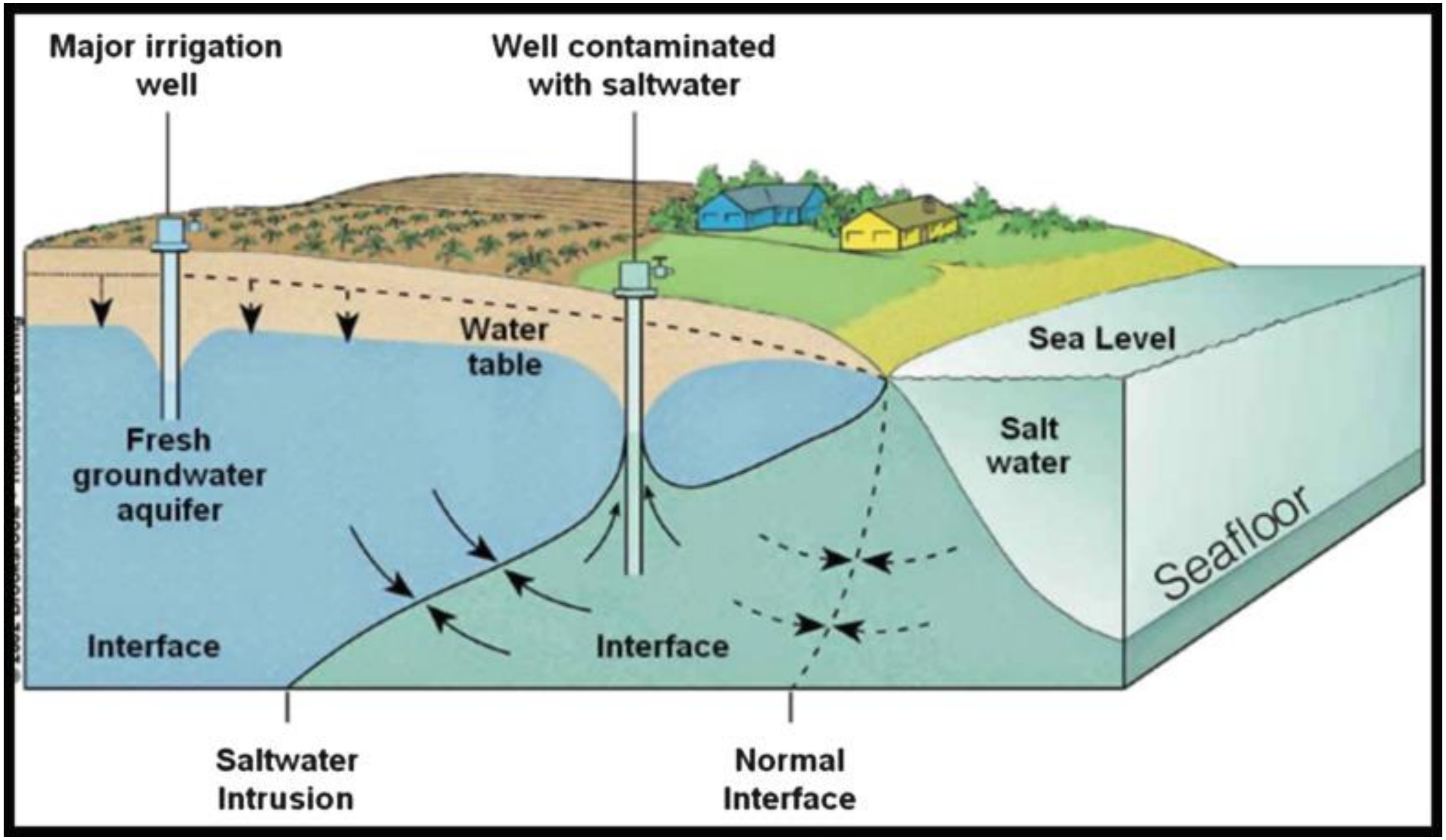

Overabstraction and saltwater intrusion

Time series hydro-geochemical quality of nearby aquifers

Parameter	Unit	WHO's Standard (S_i)	Weight of each parameter (w_i)	Relative Weight (Wi)
SO_4^{2-}	mg/L	250	4	0.121
Cl^-	mg/L	250	3	0.091
HCO_3^-	mg/L	500	3	0.091
pH	-	6.5-8.5	4	0.121
EC	us/cm	500	4	0.121
TDS	mg/L	500	5	0.152
TH	mg/L	500	3	0.091
K^+	mg/L	12	2	0.061
Na^+	mg/L	200	2	0.061
Mg^{2+}	mg/L	50	1	0.030
Ca^{2+}	mg/L	75	2	0.061

Spearman correlation results between WQI and variables

Variables	Tasuj	Shabestar	Tabriz(a)	Tabriz(b)	Shiramin	Azarshahr	Maragheh	Ajabshir	MiandoAb
SO_4^{2-}	0.427	0.850	0.910	0.768	0.839	0.652	0.817	0.850	0.782
Cl^-	0.836	0.968	0.964	0.685	0.909	0.916	0.937	0.937	0.868
HCO_3^-	0.273	0.559	0.636	0.565	0.205	0.491	0.522	0.499	0.780
CO_3^{2-}	-0.401	-0.464	-0.573	-0.144	-0.268	-0.126	-0.077	-0.046	0.200
anion	0.960	0.960	0.969	0.832	0.911	0.952	0.968	0.956	0.952
pH	-0.384	-0.620	-0.459	-0.402	-0.465	-0.362	0.193	0.048	0.150
TDS	0.971	0.958	0.977	0.803	0.912	0.955	0.960	0.948	0.946
TH	0.822	0.881	0.924	0.785	0.881	0.948	0.909	0.892	0.788
EC	0.971	0.960	0.803	0.606	0.660	0.696	0.853	0.876	0.908
SAR	0.706	0.866	0.976	0.859	0.908	0.956	0.968	0.956	0.947
K^+	0.513	0.866	0.805	0.503	0.475	0.719	0.606	0.551	0.796
Na^+	0.846	0.931	0.954	0.797	0.800	0.887	0.931	0.935	0.950
Mg^{2+}	0.747	0.914	0.946	0.781	0.901	0.921	0.908	0.906	0.834
Ca^{2+}	0.830	0.826	0.835	0.671	0.833	0.889	0.750	0.748	0.586
WQI	1	1	1	1	1	1	1	1	1

Statistical analysis of the chemical concentrations in the groundwater from 9 aquifers around the Urmia Lake

Aquifer ID: Tasuj — Aquifer area: 212.65 km^2 — Total N. of observation 1*:326 - 2*:248

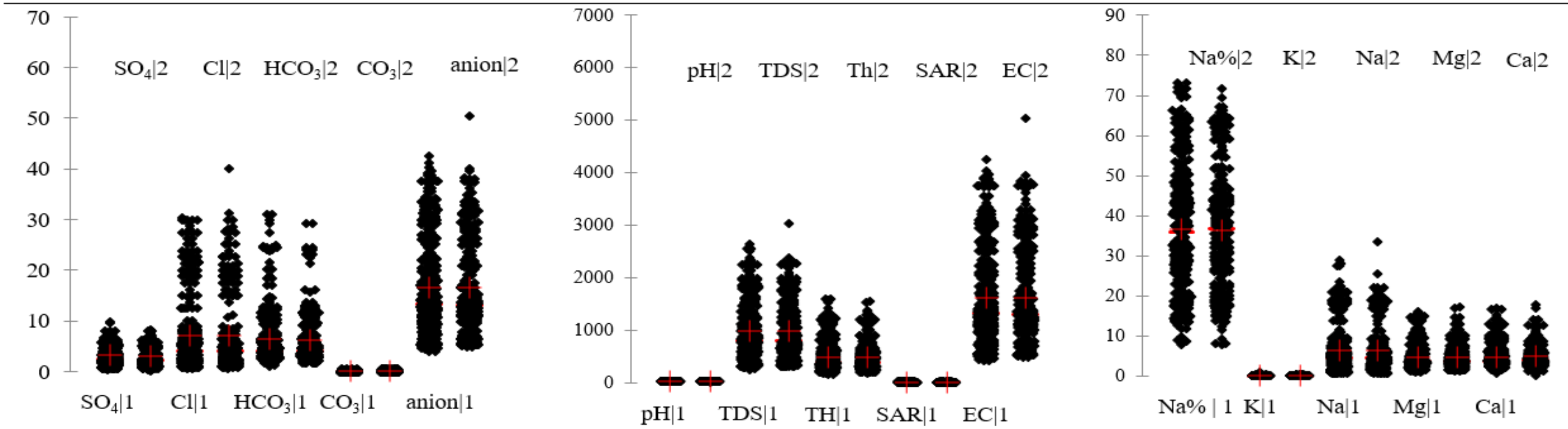

Aquifer ID: Shabestar-Sufian — Aquifer area: 479.33 km^2 — Total N. of observation 1*:576 - 2*:410

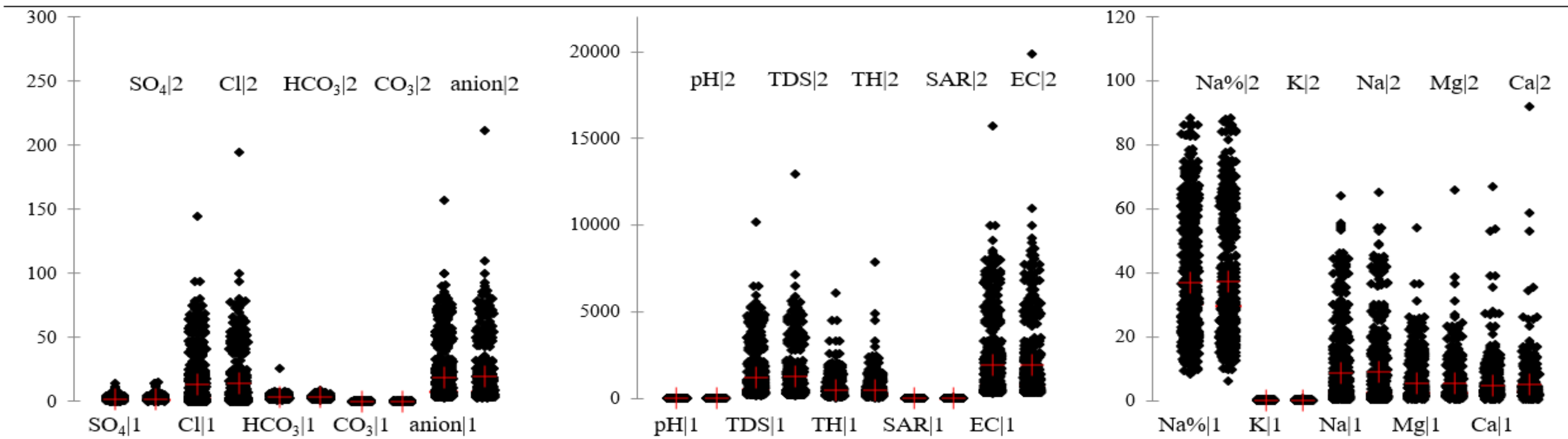

PCA analysis of 800 wells in nine aquifers and two dry and rainy seasons during the 20-year study period with fourteen quality variables combined with cluster analysis results (Zone A to E)

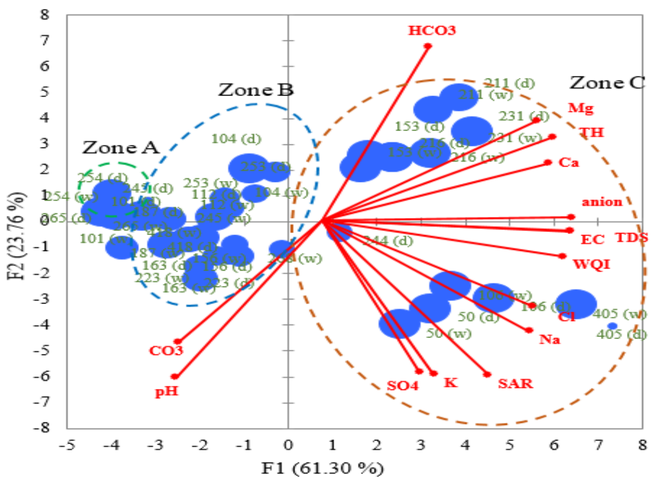

Observations (axes F1 and F2: 85.06 %)

Tasuj

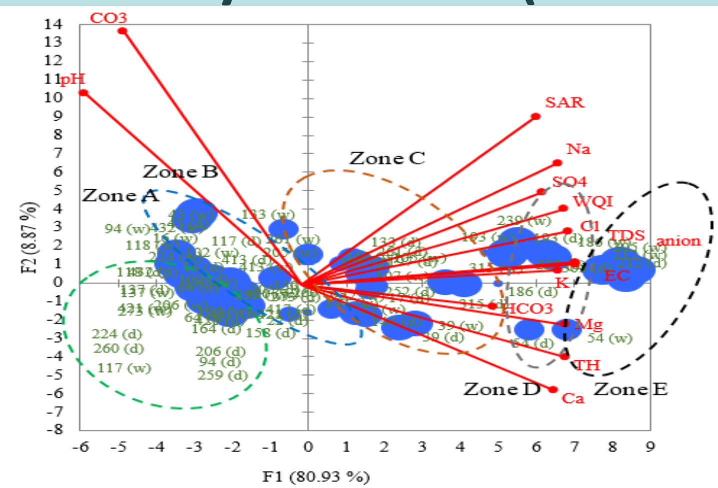

Observations (axes F1 and F2: 89.80 %)

Shabestar

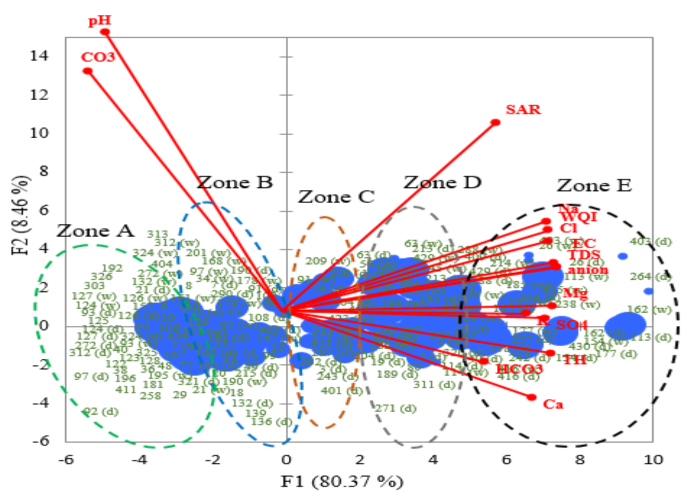

Observations (axes F1 and F2: 88.83 %)

Tabriz (a)

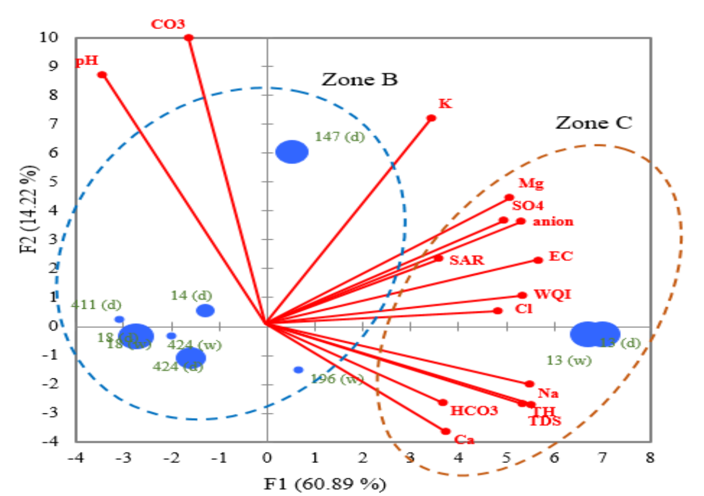

Observations (axes F1 and F2: 75.11 %)

Tabriz (b)

A GIS-based spatiotemporal impact assessment of droughts in the hyper-saline Urmia Lake Basin on the hydro-geochemical quality of nearby aquifers

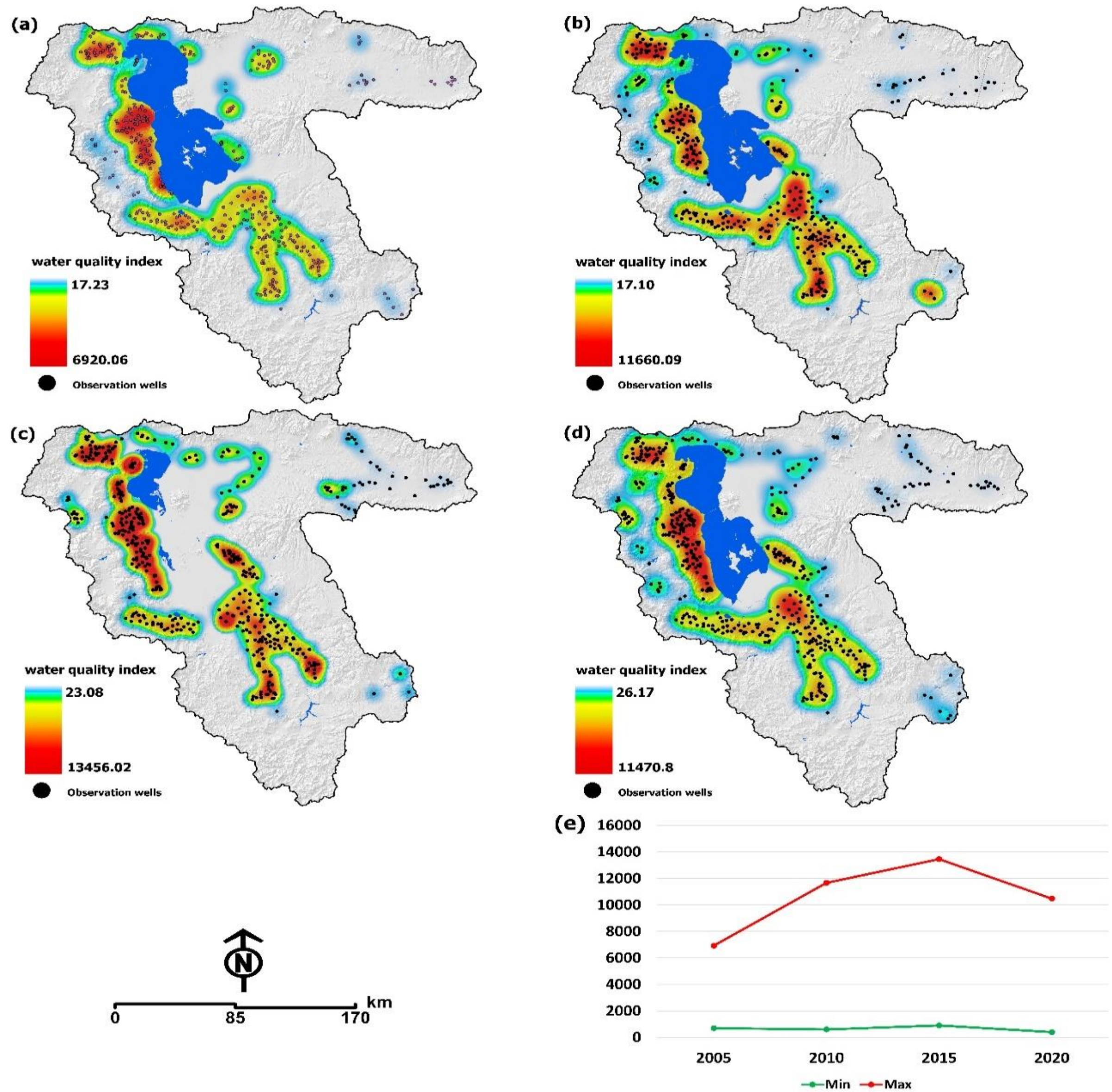

Scenario based food security mapping

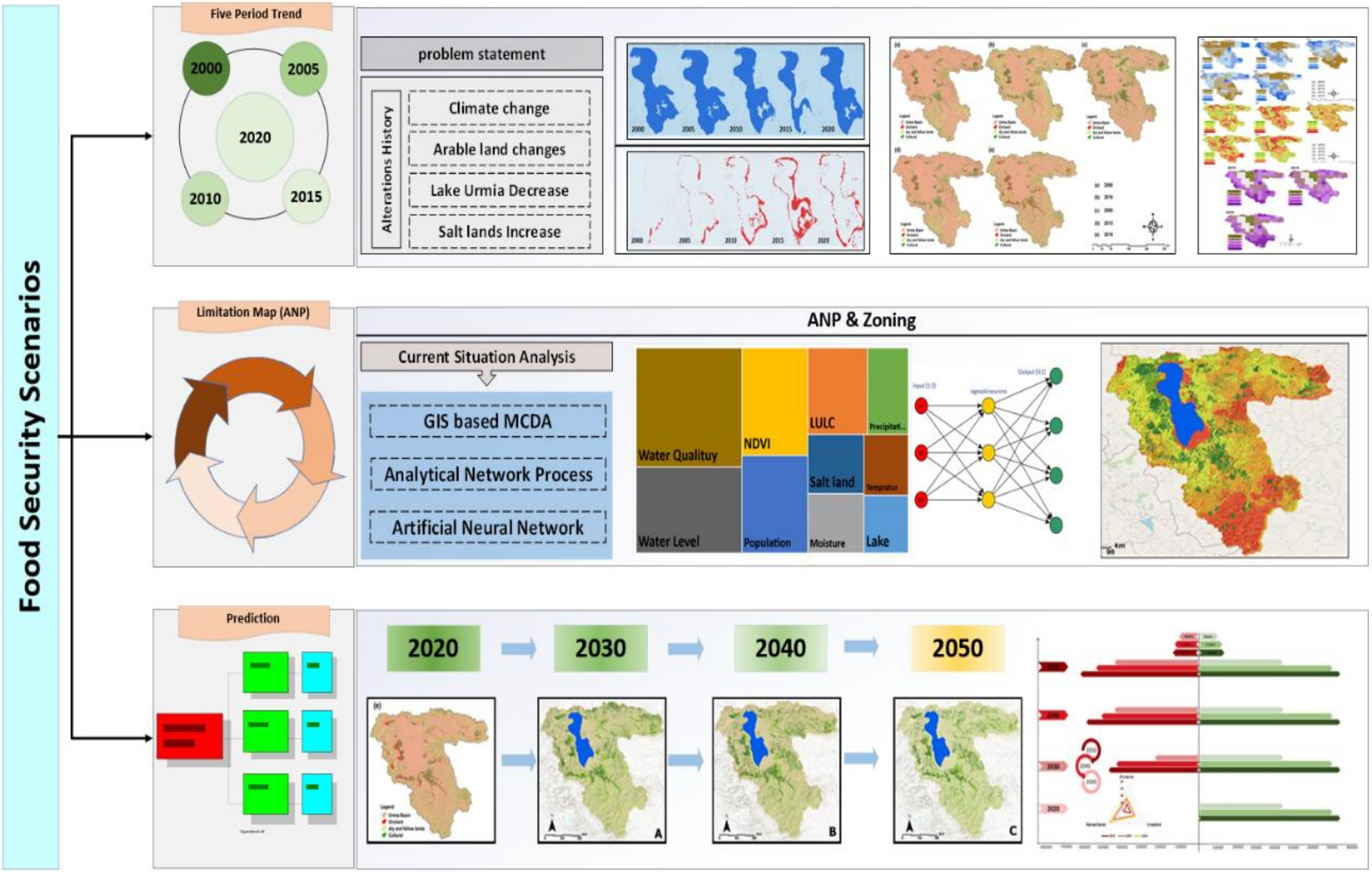

Results of simulation using a CA- Markov: aquifer salinization for 2030 (a), 2040(b), 2050 (c) and soil salinization for 2030 (d), 2040 (e) and 2050 (f)

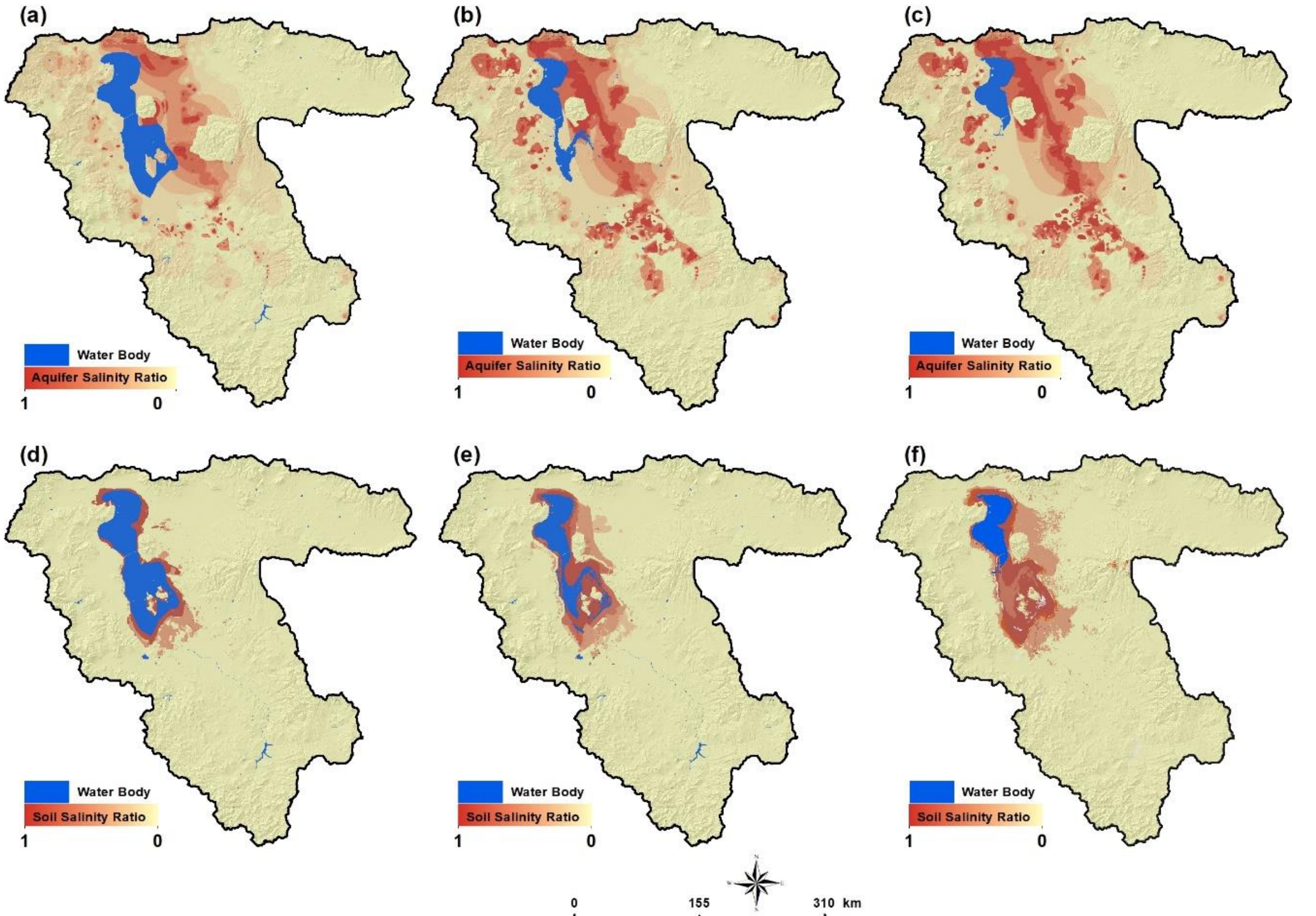

Spatial distribution of the selected indicators for SFP mapping

a) Precipitation
b) Temperature
c) Humidity
d) Sunshine hours
e) Groundwater
f) Depth
g) Water quality
h) Soil degradation
i) Soil fertility
j) Soil texture
k) salt scattering spots
l) Land use/cover
m) Soil depth

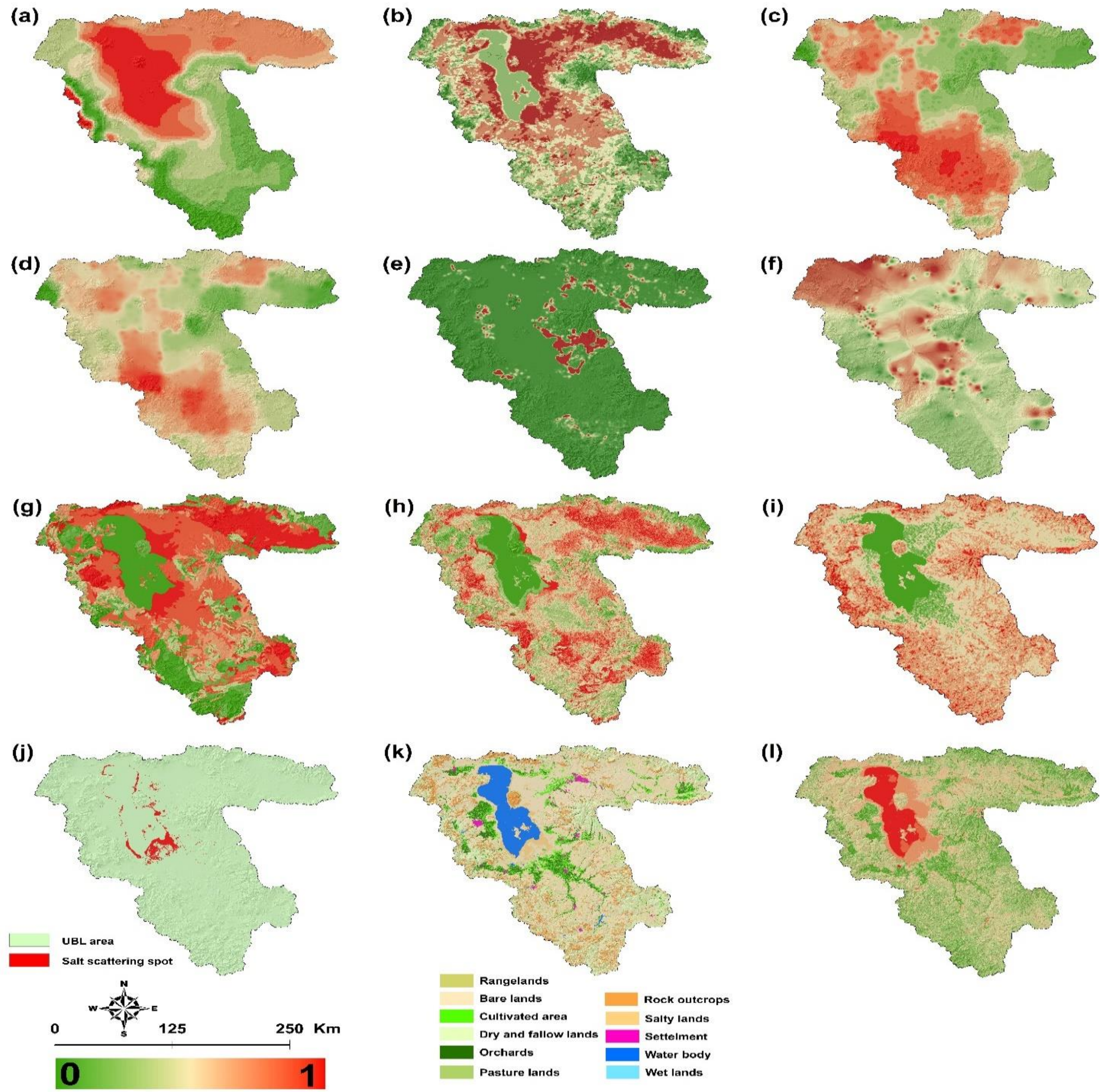

Scenario based food security mapping

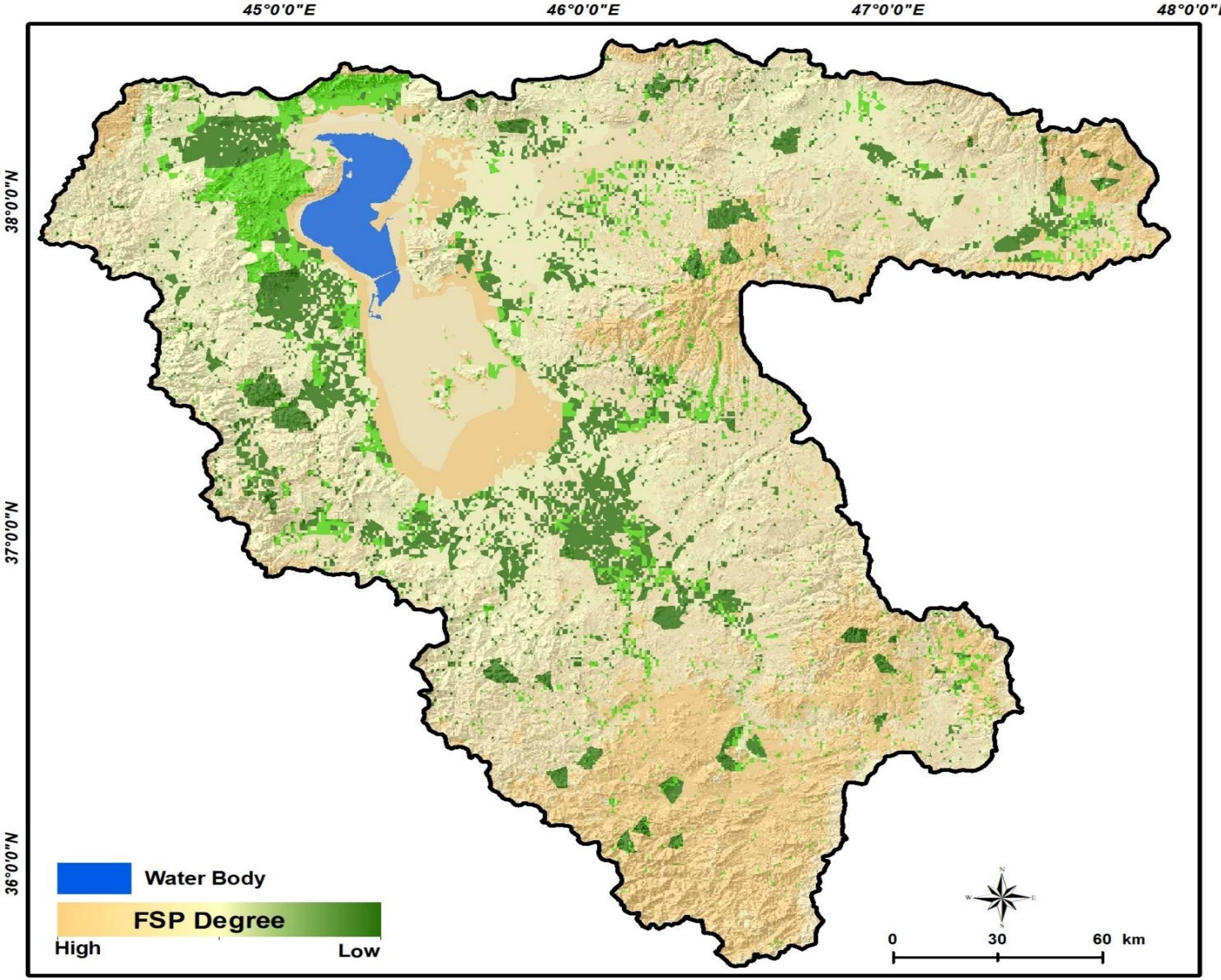

Results of the scenario-based FSP in spatial correlation with aquifer salinization (a) and soil salinity (b) in 2050

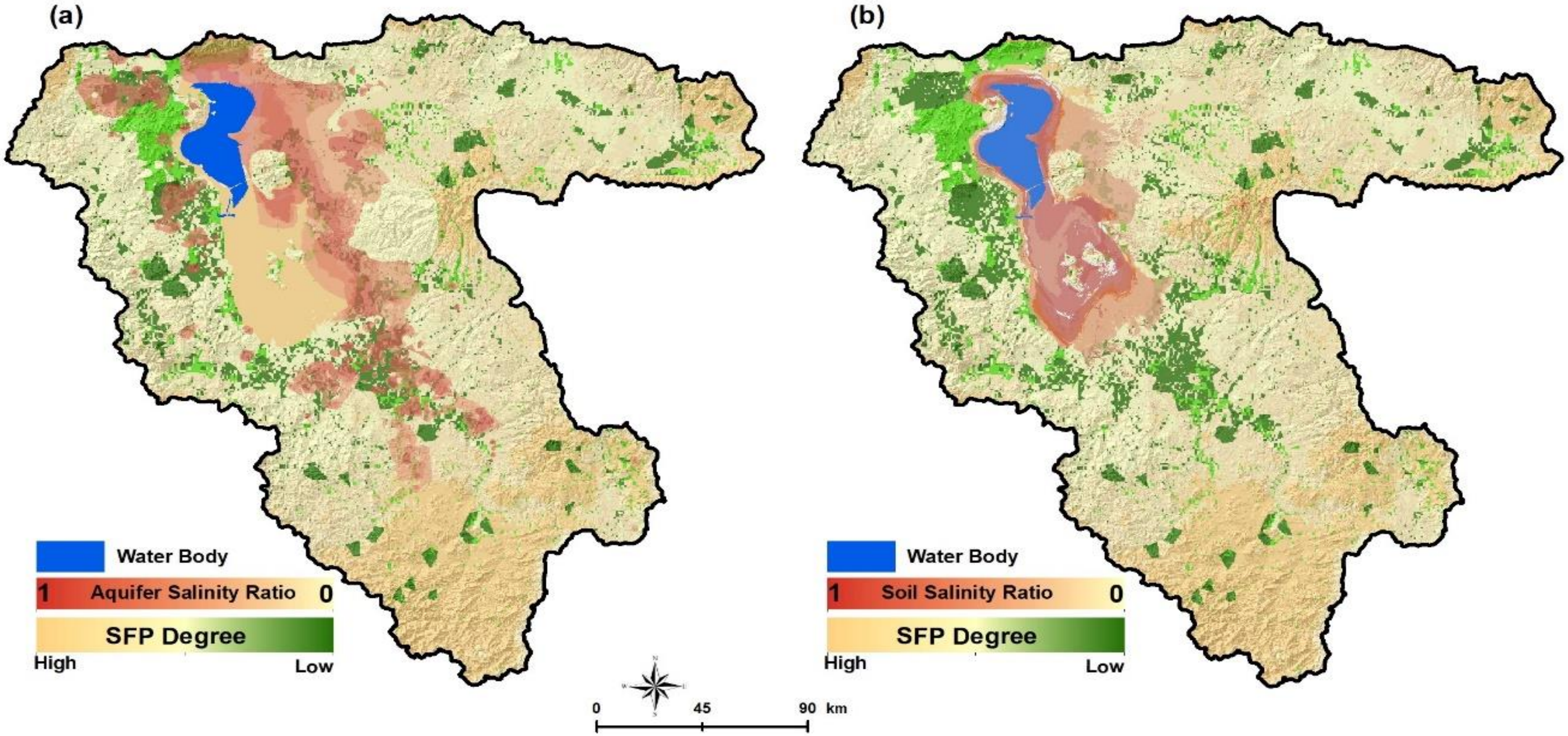

Results of the scenario-based FSP

Hectares	2030		2040		2050	
Farmlands impacted by aquifer salinization	29,100	7.8 %	248,000	66 %	260,200	69.38 %
Farmlands impacted by soil salinization	20,600	5.49 %	52,000	13.87 %	132,420	35.4 %

The LUB area currently produces 8.47% of the total food produced in Iran and feeds 7.3 million people

Annual average of major craps produced in the ULB and their contribution for food system of the country

Horticultural products	Apricot	11,250	7.8
	Appel	995,000	21.4
	Grape	485,200	11.1
	Peach & nectarines	654,200	6.2
	Walnut	34,525	8.7
	Cherries	15,401	3.2
	Almond	27,235	7.5
livestock products	Red meat	71,550	11.2
	White meat	98,520	4.8
	Egg	96,245	11.4
	Milk	758,950	10.8
	Honey	25,500	16.9
	Fish	7,852	2.3
	Sum	5,710,022	

A scenario-based food security analysis and halophyte crop suitability assessment

Based on the critical environmental condition and soil salinization, some halophyte plants can be cultivated as native plant in the salty lands.

Salicornia/ Queller

Soil salinity analysis for Salicornia cultivation: Field analysis

Soil salinity analysis for Salicornia cultivation

Physiochemical laboratory analysis for soil sampling analysis in LUB

Analysis	Min	Mean	Max	Standard Deviation (σ)	Coefficient of Variation
Sand (%)	7.7	42.3	90.0	26.9	0.64
Silt (%)	1.3	31.8	58.7	16.2	0.51
Clay (%)	5.6	25.7	51.2	14.2	0.55
Organic compounds (%)	0.0	1.4	4.3	1.5	1.09
Specific Gravity (g/cm3)	2.1	2.3	2.4	0.08	0.04
CaCO3(%)	5.2	16.4	30.2	6.27	0.38
pH	7.7	8.0	8.6	0.29	0.04
ECe (dS/m)	0.8	2.5	4.8	1.4	0.58
Sodium absorption ratio	1.9	14.7	44.4	13.9	0.95
Exchangeable Sodium Percentage	17.17	27.16	50.32	13.9	0.51
ESP2	15.37	31.89	40.81	13.9	0.44

A scenario-based food security analysis and halophyte crop suitability assessment: Laboratory analysis

Some properties of European Salicornia in comparison			
European Salicornia	View	Taste	Smell
Run 1 **(Humboldt University of Berlin-** **Berlin (HU)**	Dark green, soft	Salty, crunchy, refreshing	Neutral
Run 2 **Low salinity in irrigation** **(HU-Berlin)**	Dark green, soft	Slightly less salty, slightly peppery, crisp, refreshing,	Neutral
Zeekraal (commercially for sale)	Slightly darker green, solid	Slightly saltier, slightly fishy, firm to the bite	Neutral

A scenario-based food security analysis and halophyte crop suitability assessment: Laboratory analysis

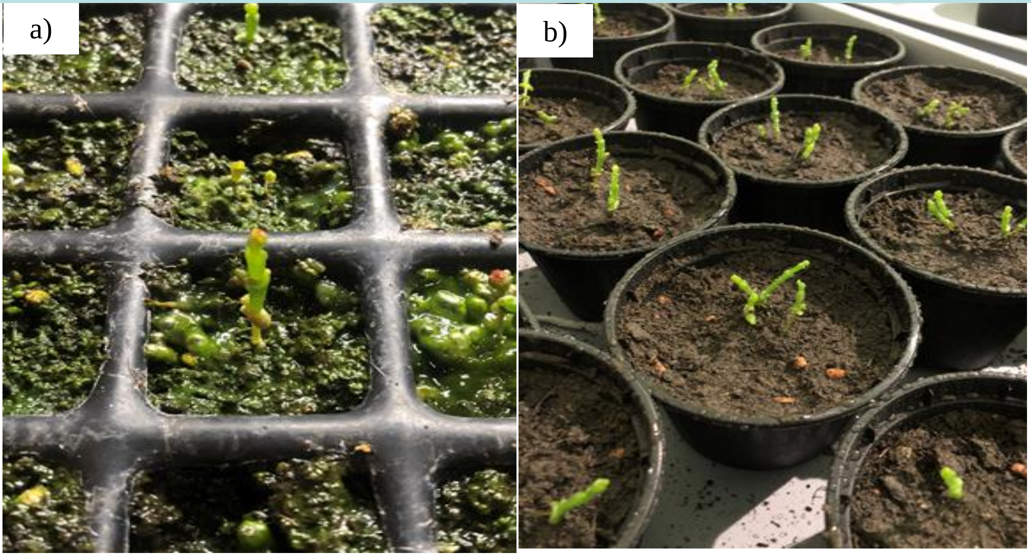

Laboratory growth and propagation of European Salicornia in trays after 32 days

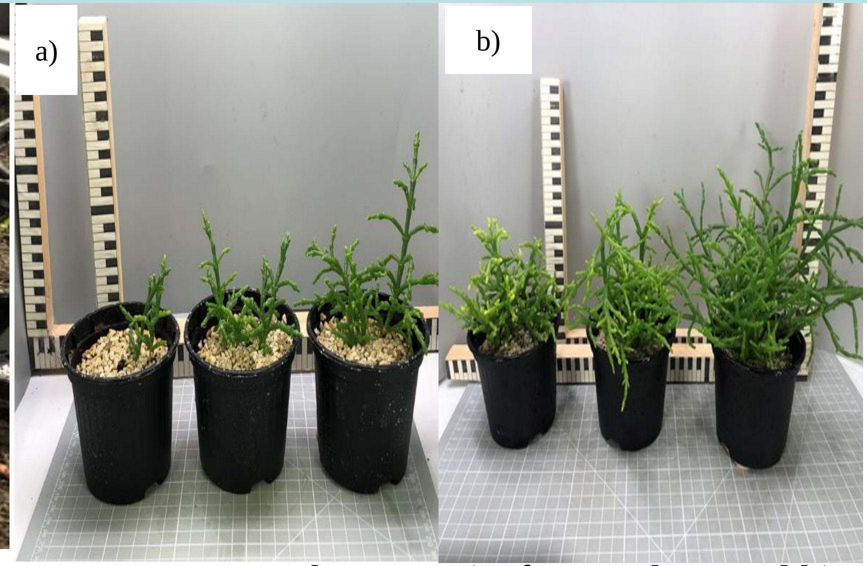

European *Salicornia* a) after 21 days and b) after 35 days of growth

Simulated European *Salicornia* in the LUB in different growth stages

A scenario-based food security analysis and halophyte crop suitability assessment: Research Methodology

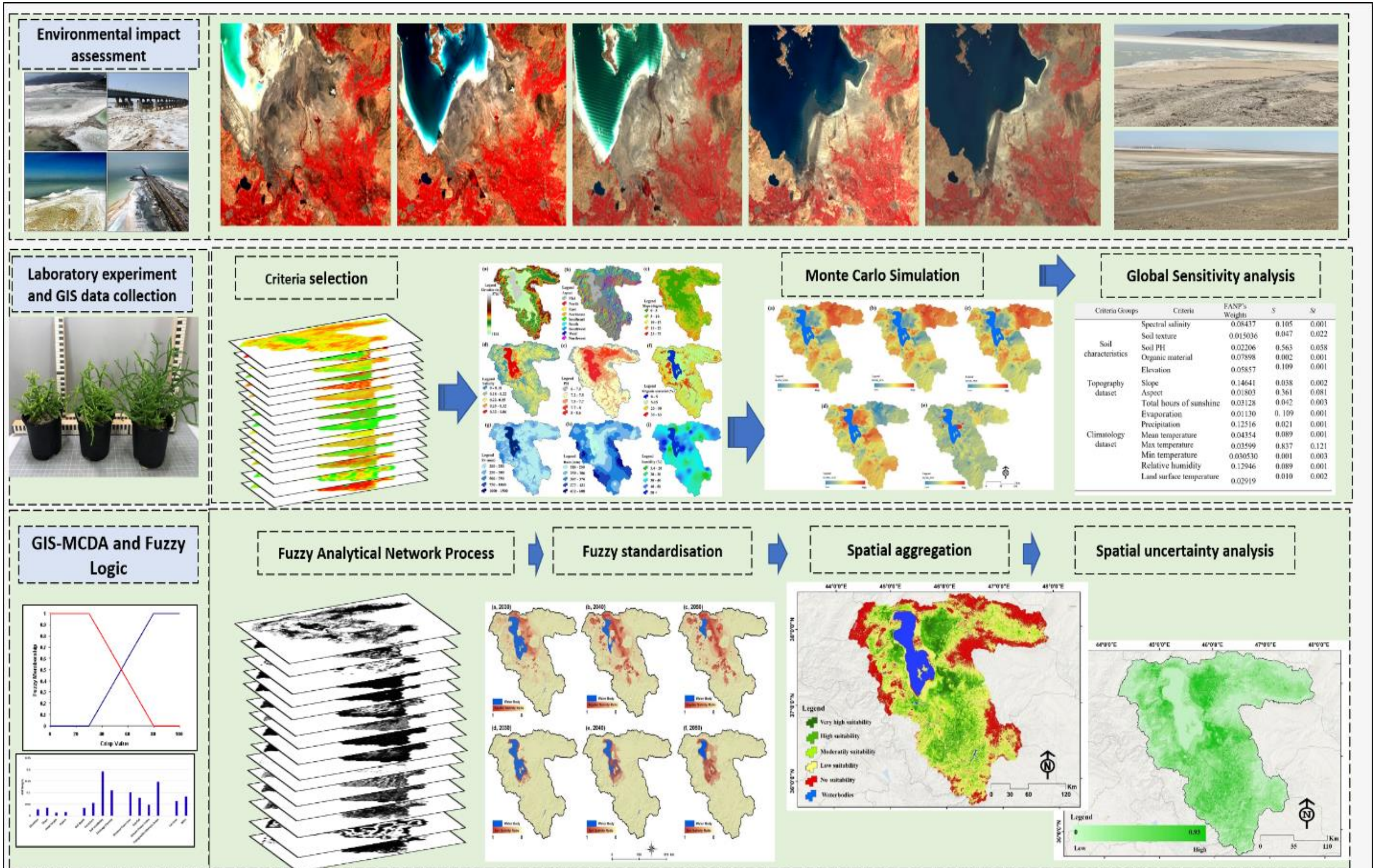

Criteria Groups	Criteria	FANP's Weights	S	St
Soil characteristics	Spectral salinity	0.08437	0.105	0.001
	Soil texture	0.015036	0.047	0.022
	Soil PH	0.02206	0.563	0.058
	Organic material	0.07898	0.002	0.001
	Elevation	0.05857	0.109	0.001
Topography dataset	Slope	0.14641	0.038	0.002
	Aspect	0.01803	0.361	0.081
Climatology dataset	Total hours of sunshine	0.03128	0.042	0.003
	Evaporation	0.01130	0. 109	0.001
	Precipitation	0.12516	0.021	0.001
	Mean temperature	0.04354	0.089	0.001
	Max temperature	0.03599	0.837	0.121
	Min temperature	0.030530	0.001	0.003
	Relative humidity	0.12946	0.089	0.001
	Land surface temperature	0.02919	0.010	0.002

GIS spatial decision making systems applied to Salicornia land suitability analysis

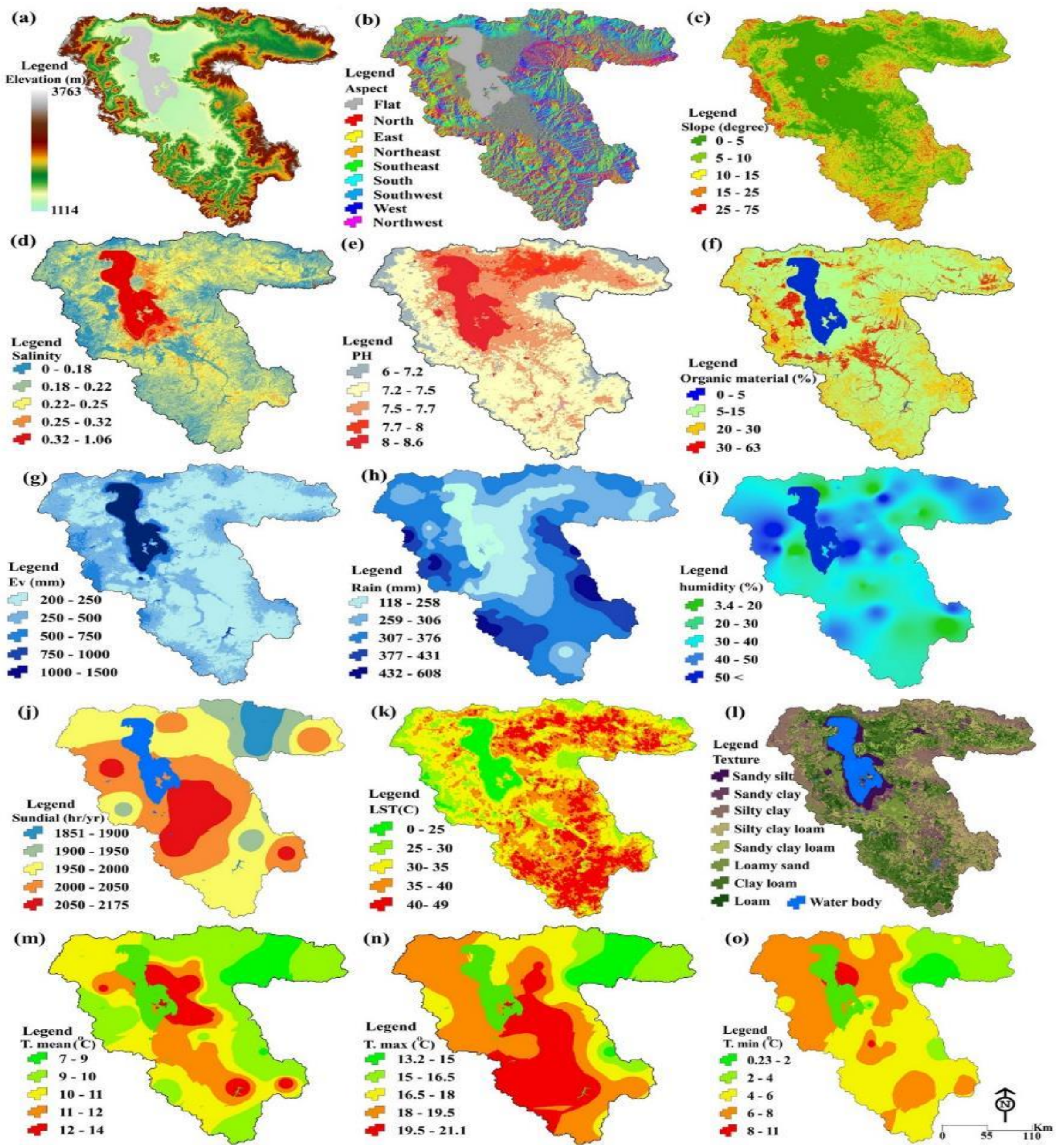

- a) elevation,
- b) aspect
- c) slope
- d) soil salinity EC,
- e) soil pH
- f) soil organic material
- g) evaporation
- h) precipitation,
- i) humidity
- j) sun hours,
- k) Land surface temperature
- l) soil texture
- m) mean temperature,
- n) max temperature and
- o) min temperature

A scenario-based food security analysis and halophyte crop suitability assessment: Criteria weighting and sensitivity analysis

Main Criteria	Criteria	FANP's Weights	*S*	*St*
Soil characteristics	Spectral salinity	0.08437	0.105	0.001
	Soil texture	0.015036	0.047	0.022
	Soil PH	0.02206	0.563	0.058
	Organic material	0.07898	0.002	0.001
Topography dataset	Elevation	0.05857	0.109	0.001
	Slope	0.14641	0.038	0.002
	Aspect	0.01803	0.361	0.081
Climatology dataset	Total hours of sunshine	0.03128	0.042	0.003
	Evaporation	0.01130	0. 109	0.001
	Precipitation	0.12516	0.021	0.001
	Mean temperature	0.04354	0.089	0.001
	Max temperature	0.03599	0.837	0.121
	Min temperature	0.030530	0.001	0.003
	Relative humidity	0.12946	0.089	0.001
	Land surface temperature (LST)	0.02919	0.010	0.002

A scenario-based food security analysis and halophyte crop suitability assessment: Results

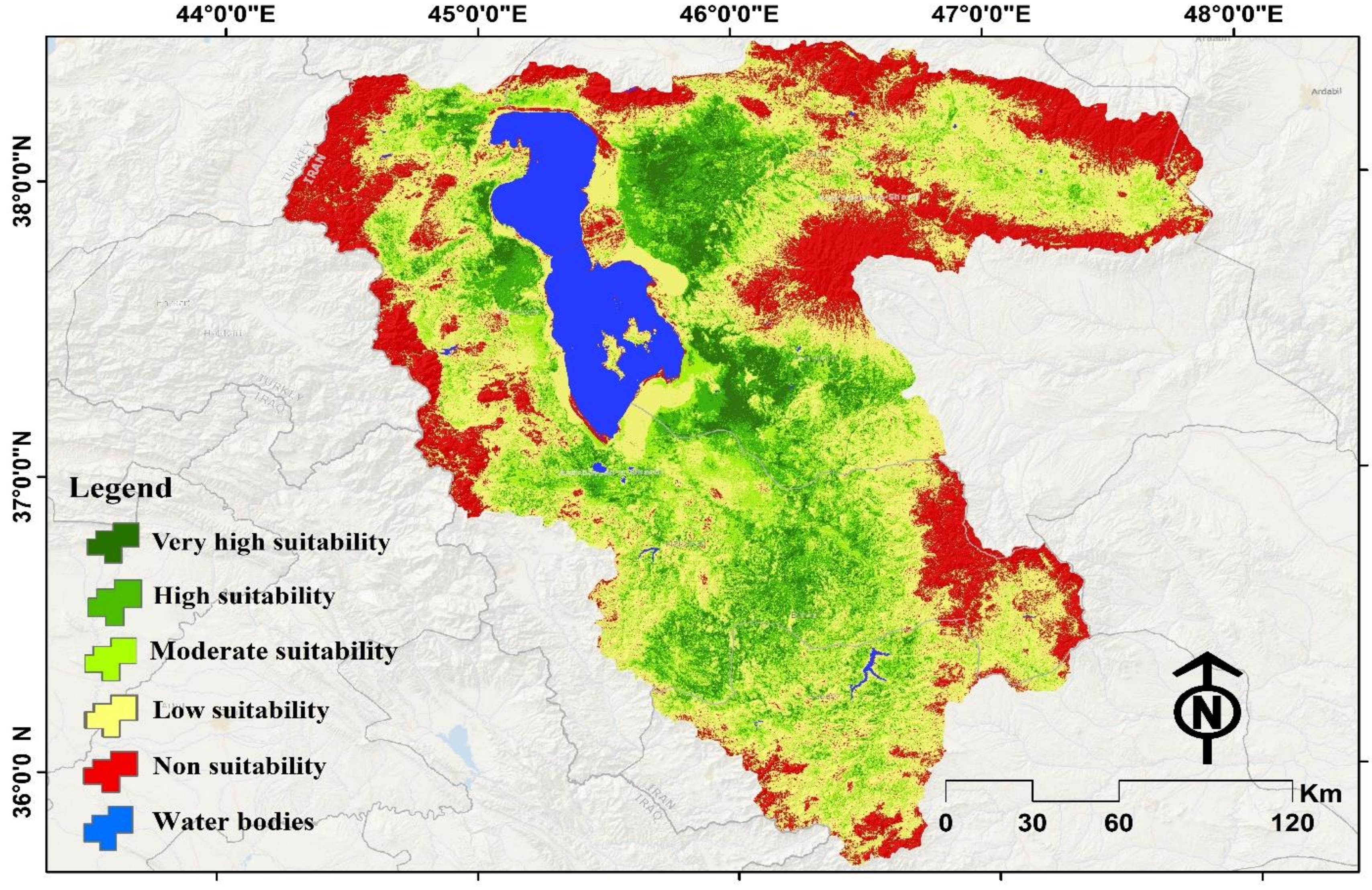

Health effects of shrinking hyper-saline lakes: spatiotemporal modeling of the Lake Urmia drought on the local population

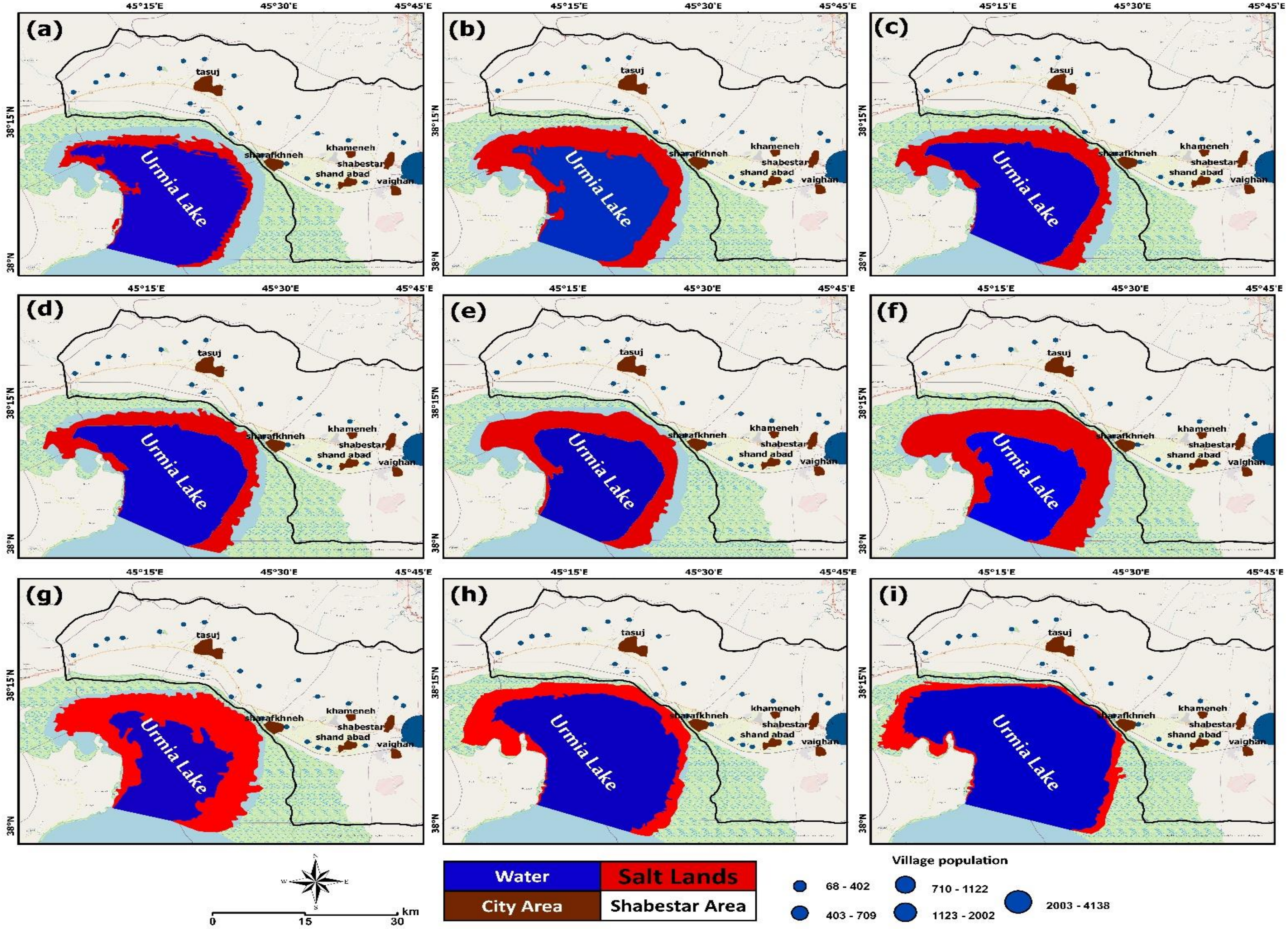

Health effects of shrinking hyper-saline lakes: spatiotemporal modeling of the Lake Urmia drought on the local population

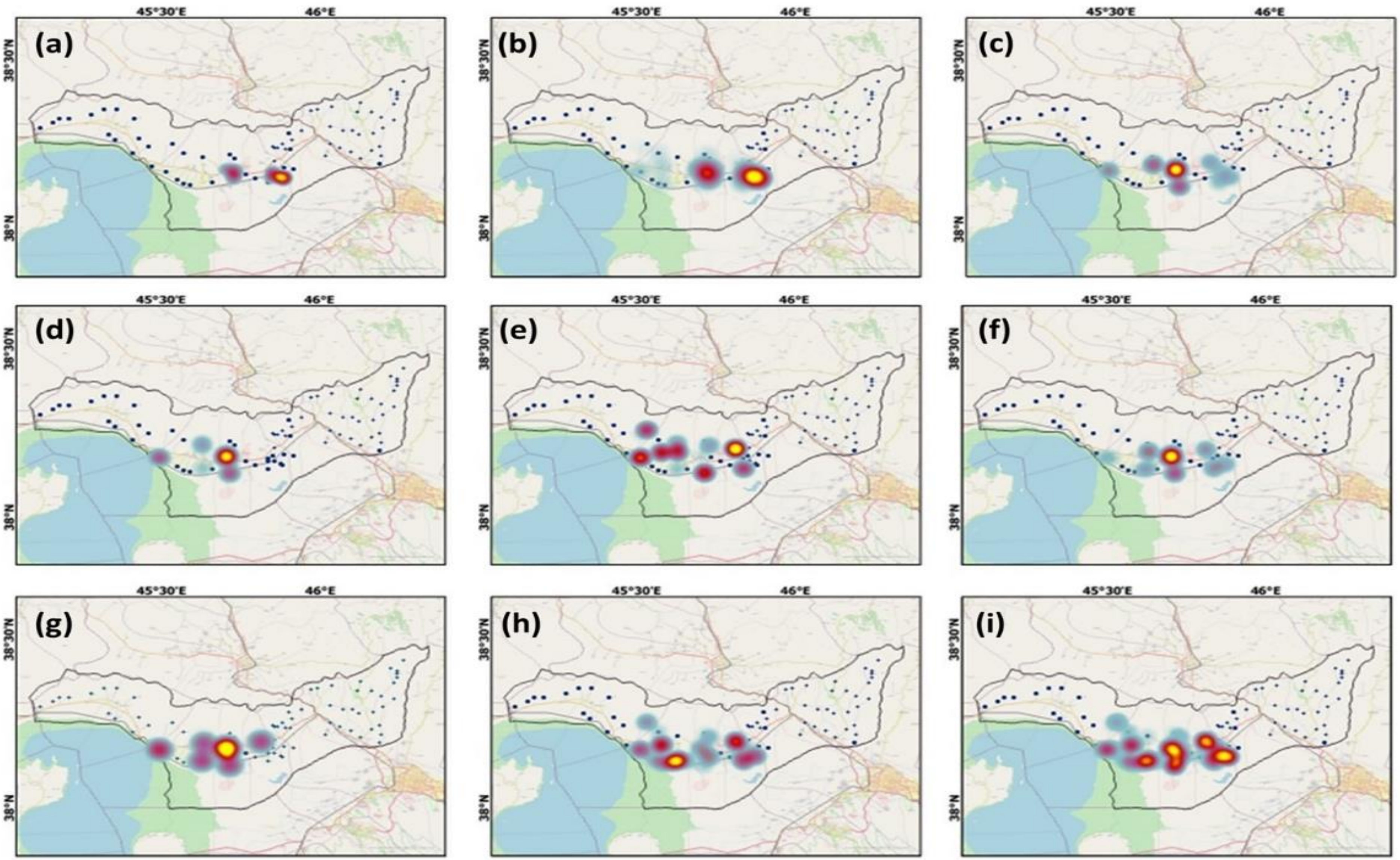

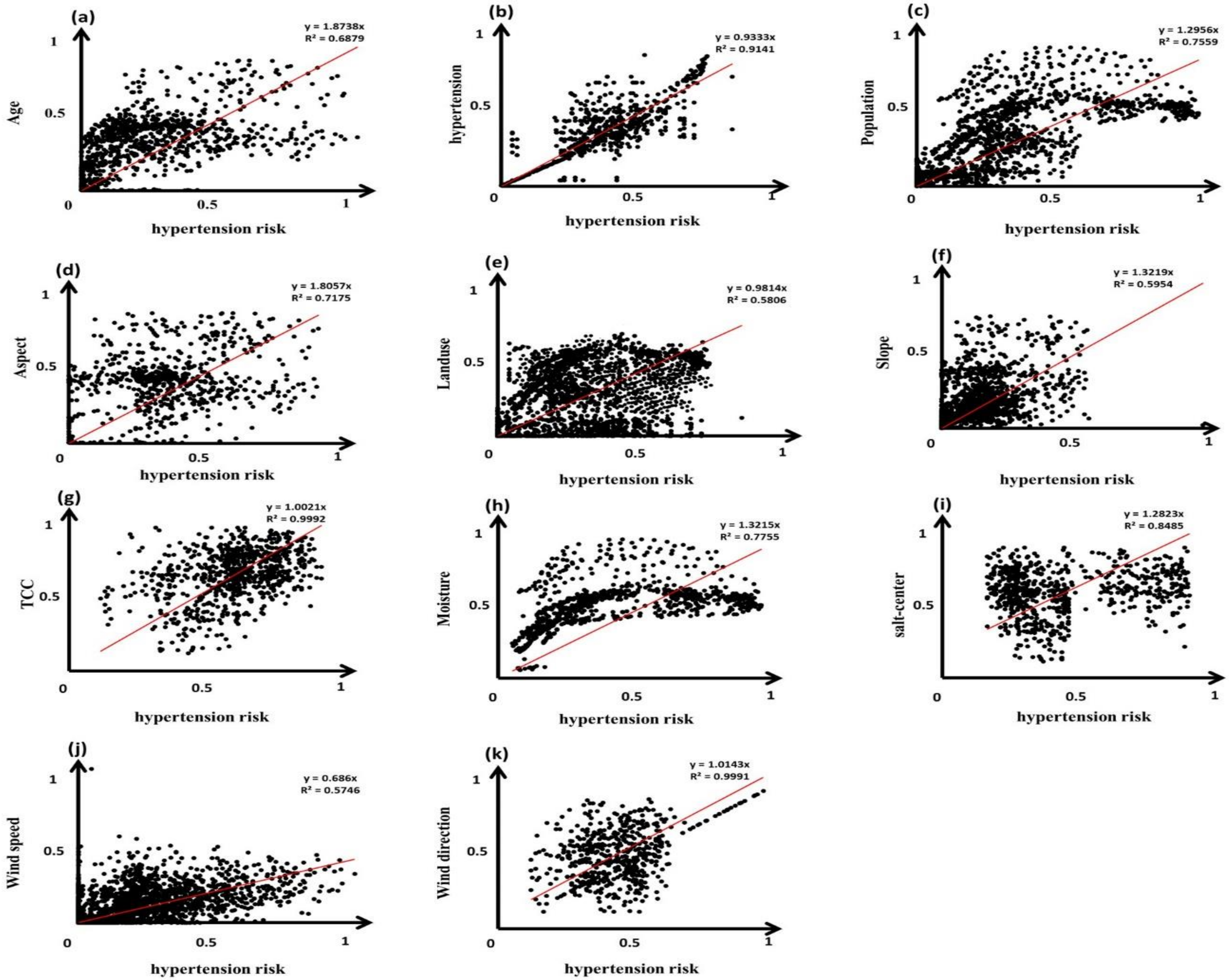

Results of the spatial correlation of the aggregated average hypertension map with the selected criteria for health vulnerability and risk mapping: a) Age group, b) Current status of hypertension, c) Population density, d) Slope-aspect, e) Land use/cover, f) Slope, g) Vegetation continuous fields), h) Moisture, i) Distance to salt-centers, j) Wind speed, and k) Wind direction. These plots indicate the contribution of each criterion to the vulnerability and health risk.

A GIS based modeling of the Lake Urmia drought on the local population

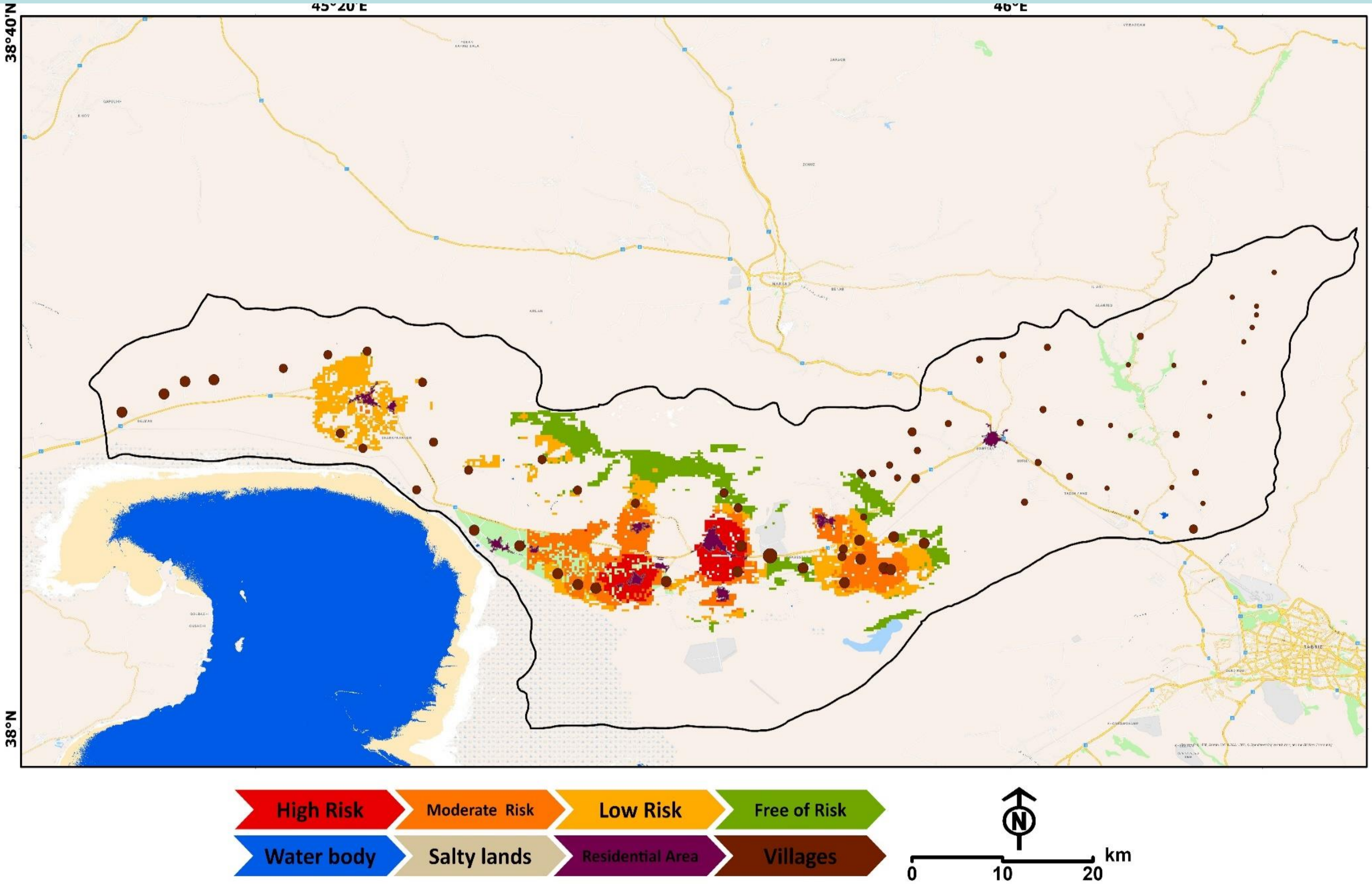

Taylor & Francis
Taylor & Francis Group

GIScience & Remote Sensing

ISSN: (Print) (Online) Journal homepage: https://www.tandfonline.com/loi/tgrs20

A comparison of the integrated fuzzy object-based deep learning approach and three machine learning techniques for land use/cover change monitoring and environmental impacts assessment

Bakhtiar Feizizadeh, Keyvan Mohammadzade Alajujeh, Tobia Lakes, Thomas Blaschke & Davoud Omarzadeh

To cite this article: Bakhtiar Feizizadeh, Keyvan Mohammadzade Alajujeh, Tobia Lakes, Thomas Blaschke & Davoud Omarzadeh (2021): A comparison of the integrated fuzzy object-based deep learning approach and three machine learning techniques for land use/cover change monitoring and environmental impacts assessment, GIScience & Remote Sensing, DOI: 10.1080/15481603.2021.2000350

To link to this article: https://doi.org/10.1080/15481603.2021.2000350

Routledge
Taylor & Francis Group

Journal of Environmental Planning and Management

ISSN: (Print) (Online) Journal homepage: https://www.tandfonline.com/loi/cjep20

Machine learning data-driven approaches for land use/cover mapping and trend analysis using Google Earth Engine

Bakhtiar Feizizadeh, Davoud Omarzadeh, Mohammad Kazemi Garajeh, Tobia Lakes & Thomas Blaschke

To cite this article: Bakhtiar Feizizadeh, Davoud Omarzadeh, Mohammad Kazemi Garajeh, Tobia Lakes & Thomas Blaschke (2021): Machine learning data-driven approaches for land use/cover mapping and trend analysis using Google Earth Engine, Journal of Environmental Planning and Management, DOI: 10.1080/09640568.2021.2001317

To link to this article: https://doi.org/10.1080/09640568.2021.2001317

Get Access

Outline

ELSEVIER
CATENA
Volume 207, December 2021, 105585

A deep learning convolutional neural network algorithm for detecting saline flow sources and mapping the environmental impacts of the Urmia Lake drought in Iran

Bakhtiar Feizizadeh [a, b], Mohammad Kazemi Garajeh [a], Tobia Lakes [c], Thomas Blaschke [b]

Show more

Add to Mendeley Share Cite

https://doi.org/10.1016/j.catena.2021.105585 Get rights and content

remote sensing

Submit to this Journal
Review for this Journal
Edit a Special Issue

Article Menu

Article Overview

- Abstract
- Open Access and Permissions
- Share and Cite
- Article Metrics
- Order Article Reprints

Open Access Article

Impacts of the Urmia Lake Drought on Soil Salinity and Degradation Risk: An Integrated Geoinformatics Analysis and Monitoring Approach

by Bakhtiar Feizizadeh [1,2,*], Davoud Omarzadeh [3], Keyvan Mohammadzadeh Alajujeh [1], Thomas Blaschke [4] and Mohsen Makki [2]

1 Department of Remote Sensing and GIS, University of Tabriz, Tabriz 51368, Iran
2 Department of Geography, Humboldt-Universität zu Berlin, 10099 Berlin, Germany
3 IN3, Universitat Oberta de Catalunya, 08018 Barcelona, Spain
4 Department of Geoinformatics (Z-GIS), University of Salzburg, 5020 Salzburg, Austria
* Author to whom correspondence should be addressed.

Academic Editors: Valerio Tramutoli, Francesco Marchese, Nicola Genzano and Carolina Filizzola

remote sensing

Submit to this Journal

Review for this Journal

Edit a Special Issue

Article Menu

Article Overview

- Abstract
- Open Access and Permissions
- Share and Cite
- Article Metrics

Open Access Article

A GIS-Based Spatiotemporal Impact Assessment of Droughts in the Hyper-Saline Urmia Lake Basin on the Hydro-Geochemical Quality of Nearby Aquifers

by Bakhtiar Feizizadeh [1,2,*], Zahra Abdollahi [3] and Behzad Shokati [4]

1 Applied GISciences Lab, Department of Geography, Humboldt-Universität zu Berlin, 10781 Berlin, Germany

2 Department of Remote Sensing and GIS, University of Tabriz, Tabriz 51368, Iran

3 Soil Conservation and Watershed Management Research Department, Zanjan Agricultural and Natural Resources Research and Education Center, AREEO, Zanjan 45131, Iran

4 Young Researchers and Elite Club, Maragheh Branch, Islamic Azad University, Maragheh 55131, Iran

* Author to whom correspondence should be addressed.

sensors

Submit to this Journal

Review for this Journal

Edit a Special Issue

Article Menu

Article Overview

- Abstract
- Supplementary Material
- Open Access and Permissions
- Share and Cite

Open Access Article

QADI as a New Method and Alternative to Kappa for Accuracy Assessment of Remote Sensing-Based Image Classification

by Bakhtiar Feizizadeh [1,2,*], Sadrolah Darabi [1], Thomas Blaschke [3] and Tobia Lakes [2,4]

1 Department of Remote Sensing and GIS, University of Tabriz, Tabriz 516661647, Iran

2 GIScience Lab, Humboldt-Universität zu Berlin, 10117 Berlin, Germany

3 Department of Geoinformatics-Z-GIS, University of Salzburg, 5020 Salzburg, Austria

4 IRI THESys, Humboldt-Universität zu Berlin, 10117 Berlin, Germany

* Author to whom correspondence should be addressed.

Academic Editors: Andrea Facchinetti and Paul Harris

Sensors **2022**, 22(12), 4506; https://doi.org/10.3390/s22124506

scientific reports

View all journals | Search | Log in

Explore content | About the journal | Publish with us | Sign up for alerts | RSS feed

nature > scientific reports > articles > article

Article | Open Access | Published: 14 April 2022

Scenario-based analysis of the impacts of lake drying on food production in the Lake Urmia Basin of Northern Iran

Bakhtiar Feizizadeh, Tobia Lakes, Davoud Omarzadeh, Ayyoob Sharifi, Thomas Blaschke & Sadra Karimzadeh

Scientific Reports **12**, Article number: 6237 (2022) | Cite this article

2838 Accesses | **11** Citations | **32** Altmetric | Metrics

Abstract

Download PDF

Associated Content

Collection

Top 100 in Sustainability - 2022

Sections | Figures | References

Abstract

Introduction

Discussion

scientific reports

View all journals | Search | Log in

Explore content | About the journal | Publish with us | Sign up for alerts | RSS feed

nature > scientific reports > articles > article

Article | Open Access | Published: 28 January 2023

Health effects of shrinking hyper-saline lakes: spatiotemporal modeling of the Lake Urmia drought on the local population, case study of the Shabestar County

Bakhtiar Feizizadeh, Tobia Lakes, Davoud Omarzadeh & Samira Pourmoradian

Scientific Reports **13**, Article number: 1622 (2023) | Cite this article

1118 Accesses | **12** Altmetric | Metrics

Abstract

Download PDF

Sections | Figures | References

Abstract

Introduction

Study area

Dataset and methods

Methodology

Results

Discussion

Submissions Being Processed for Author

Page: 1 of 1 (1 total submissions) Results per page 10

Action	Manuscript Number	Title	Initial Date Submitted	Status Date	Current Status
View Submission View Reference Checking Results Send E-mail	LUP-D-23-00170	A scenario-based food security analysis and halophyte crop suitability assessment in dying lake environments impacted by climate change	Feb 03, 2023	Feb 05, 2023	With Editor

Page: 1 of 1 (1 total submissions) Results per page 10

Questions and comments are welcome!